Neurobiology of Disease 208 (2025) 106871

Contents lists available at ScienceDirect

Neurobiology of Disease

journal homepage: www.elsevier.com/locate/ynbdi

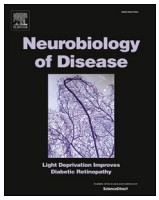

MicroRNA signature of lymphoblasts from amyotrophic lateral sclerosis patients as potential clinical biomarkers

Eva P. Cuevas [a,b,1], Enrique Madruga [a,b,1], Ignacio Valenzuela-Martínez [c], David Ramírez [c], Carmen Gil [a,b], Siranjeevi Nagaraj [d], Angeles Martin-Requero [a,b], Ana Martinez [a,b,*]

[a] Centro de Investigaciones Biológicas "Margarita Salas"-CSIC, Ramiro de Maeztu 9, 28040 Madrid, Spain
[b] Centro de Investigación Biomédica en Red en Enfermedades Neurodegenerativas, (CIBERNED), Instituto de Salud Carlos III, Av. Monforte de Lemos, 3-5, 28029 Madrid, Spain
[c] Departamento de Farmacología, Facultad de Ciencias Biológicas, Universidad de Concepción, Chile
[d] Alzheimer and other tauopathies research group, ULB Center for Diabetes Research, Medical Faculty, Université Libre de Bruxelles, ULB Neuroscience Institute, 808 route de Lennik, B-1070 Brussels, Belgium

ARTICLE INFO

Keywords:
miRNA
ALS
Biomarker
Lymphoblasts

ABSTRACT

MicroRNAs (miRNAs) are a class of small, non-coding RNAs involved in different cellular functions that have emerged as key regulators of neurodegenerative diseases such as amyotrophic lateral sclerosis (ALS). ALS is a fatal disease that lacks of not only effective treatments, but also presents delays in its diagnosis, since reliable clinical biomarkers are unavailable. In recent years, advancements in high-throughput sequencing strategies have led to the identification of novel ALS biomarkers, facilitating earlier diagnosis and assessment of treatment efficacy. Since immortalized lymphocytes obtained from peripheral blood are a suitable model to study pathological features of ALS, we employed these samples with the aim of characterize the dysregulated miRNAs in ALS patients. Next-generation sequencing (NGS) was utilized in order to analyze the expression profiles of miRNAs in immortalized lymphocytes from healthy controls, sporadic ALS (sALS), and familial ALS with mutations in superoxide dismutase 1 (SOD1-ALS). The screening analysis of the NGS data identified a set of dysregulated miRNAs, of which nine candidates were selected for qRT-PCR validation, identifying for the first time the possible importance of hsa-miR-6821-5p as a potential ALS biomarker. Furthermore, the up-regulated miRNAs identified are predicted to have direct or indirect interactions with genes closely related to ALS, such as *SIGMAR1*, *HNRNPA1* and *TARDBP*. Additionally, by Metascape enrichment analysis, we found the VEGFA/VEGFR2 signaling pathway, previously implicated in neuroprotective effects in ALS, as a candidate pathway for further analyses.

1. Introduction

Amyotrophic lateral sclerosis (ALS) is a fatal neurodegenerative disease characterized by the progressive degeneration of motor neurons, leading to muscle atrophy and paralysis (Feldman et al., 2022). Currently, there is an absence of effective treatments, and only a limited number of palliative options have been approved in certain countries. In Europe, riluzole remains the only drug in clinical use, while ultra-high doses of vitamin B12 have recently been approved in Japan (Oki et al., 2022). Furthermore, ALS exhibits significant clinical variability among patients, often resulting in diagnostic delays averaging 10 to 16 months (Lynch, 2023). There is an urgent need for the discovery of new biomarkers for ALS to accelerate accurate diagnosis, support the development of effective therapies, and enable successful patient stratification for clinical trials.

Blood-derived biomarkers have emerged as essential tools for diagnosis, prognosis, and improving clinical outcomes. Their utility stems from the minimally invasive nature of blood collection, the ease of sampling in most clinical settings, and their ability to provide early indications of disease. Additionally, they enable the monitoring of disease progression and treatment responses. This kind of biomarkers encompasses a range of molecular types, such as proteins, metabolites, and

* Corresponding author.
E-mail address: ana.martinez@csic.es (A. Martinez).
[1] Both authors contributed equally.

https://doi.org/10.1016/j.nbd.2025.106871
Received 22 January 2025; Received in revised form 25 February 2025; Accepted 11 March 2025
Available online 15 March 2025

non-coding RNAs, that may provide comprehensive information about disease mechanisms (Sturmey and Malaspina, 2022). MicroRNAs (miRNAs) are small, non-coding RNAs that play crucial roles in various cellular functions serving as key regulators in neurodegenerative diseases, including ALS (Li et al., 2023). miRNAs can be detected in blood-derived lymphocytes, serum, or plasma, providing a minimally invasive diagnostic tool (Banack et al., 2024; Nagaraj et al., 2017). Recently, high-throughput transcriptomics has significantly advanced the field as it is a cost-effective technique to analyze the complete set of RNA transcribed by specific cells or tissues under defined biological conditions (D'Agostino et al., 2022). Moreover, miRNA profiling datasets for ALS, combined with artificial intelligence approaches, have led to the development of complementary diagnostic tools that aid in the early recognition of the disease (Cheng et al., 2023).

Peripheral cells, including lymphoblastoid cell lines (LCLs) derived from ALS patients are recognized as a suitable and valuable model for accelerating drug discovery and studying different pathological pathways of ALS (Pansarasa et al., 2018). We have utilized these samples to characterize not only the miRNAs that are dysregulated in ALS patients but also to identify a reliable miRNA profile that respond to different treatments and can be used as prognostic biomarkers in future clinical trials. Recently, LCLs from ALS patients have been used to perform a transcriptional profiling of miRNA-mRNA interactions to study differences in patients with longer survival from disease onset compared with those with short survival (Waller et al., 2024), showing the utility of these cells as a source of potential biomarkers. Moreover, previous results showed that LCLs accurately represent the genetic material of the donor (Londin et al., 2011).

The goal of this work was to determine whether there are differential RNAs profiles among the well- known ALS subtypes, as this kind of information could provide additional insights into disease pathologies, and may help in diagnostic procedures and to develop personalized therapeutic treatments. In particular, we focused on the comparison of miRNA expression levels in LCLs derived from sporadic ALS patients and patients carrying mutations in the SOD1 gene, as we and others had detected distinct molecular and clinical features (Lastres-Becker et al., 2021; Mackenzie et al., 2007). We here describe the study of three different cohorts: a group of sporadic ALS subjects, a group from of *SOD1* mutations-associated ALS patients, and a neurologically normal cohort as healthy controls. We assessed the differential expression of miRNAs in easy accessible peripheral cells from patients and control individuals through next generation sequencing (NGS), and posterior qRT-PCR validation of the most significant changes in the three populations. In addition, we investigated the influence of clinical disease presentation (bulbar or spinal) in miRNAs expression levels, and the usefulness of tideglusib treatment, a GSK-3 inhibitor under clinical development for myotonic dystrophy (Horrigan et al., 2020) and effective in several ALS models (Martínez-González et al., 2021), to recover miRNAs levels in ALS cell cultures.

2. Materials and methods

2.1. Subjects

Blood samples were obtained after written informed consent. In all the cases, the privacy rights of human subjects have been observed. All patients were diagnosed by applying the revised El Escorial criteria (Ludolph et al., 2015) in the Hospital 12 de Octubre (Madrid, Spain). All procedures were in accordance with National and European Union Guidelines and approved by Institutional Review Board of Hospital 12 de Octubre (CEIC02506), and the Ethics Committee of the Spanish Council of Higher Research (protocol code 002/2020, 19 May 2021). Demographic and clinical information of control subjects and patients is presented in Table 1.

We analyzed miRNA expression using NGS in a total of 15 samples, including individuals with ALS (n = 10), comprising sALS (n = 5) and SOD1-ALS (n = 5), as well as healthy controls (n = 5). For qRT-PCR validation of the dysregulated miRNAs, the sample size was increased to a total of 25, including patients with ALS (n = 17), comprising sALS (n = 11) and SOD1-ALS (n = 6), in addition to healthy controls (n = 8).

Table 1
Demographic and clinical characteristics of participants.

Group		Code	Sex assigned at birth	Age at sample collection	Clinical presentation
Healthy controls		C100	Female	83	NA
		C105	Female	54	NA
		C106	Female	67	NA
		C108	Female	68	NA
		C110	Male	75	NA
		C112	Male	71	NA
		C123	Male	55	NA
		C124	Female	50	NA
ALS Disease	Sporadic ALS	**E2**	Female	76	Bulbar
		E4	Female	54	Bulbar
		E5	Male	54	Spinal
		E6	Female	79	Bulbar
		E8	Male	55	NK
		E10	Male	68	Bulbar
		E19.5	Male	75	Spinal
		ED5	Female	82	Bulbar
		ED8	Female	59	Spinal
		ED10	Male	67	Spinal
		ED11	Female	65	NK
	SOD1-ALS	**E11**	Female	46	Spinal
		E18.5	Male	49	Spinal
		E18.6	Female	58	Spinal
		E18.7	Male	49	Spinal
		E19.4	Male	45	Spinal
		E20.1	Female	63	NK
AD		A111	Male	76	Mild
		A121	Female	80	Moderate
		A122	Female	59	Severe
		A139	Male	68	Severe
		A140	Male	60	Severe

NA: not applicable; NK: Not known. Blue code: samples used in the NGS study.

The subjects utilized for NGS are indicated in blue, whereas for the qRT-PCR validation, all the subjects depicted in the table were employed. Samples from Alzheimer's disease (AD) patients have been used to evaluate the specificity of changes found in ALS patients in qRT-PCR analysis. The experimental outline is summarized in Fig. 1.

2.2. Establishment, culture and treatment of lymphoblastoid cell lines

Blood samples (approximately 8 mL) were obtained through antecubital vein puncture in EDTA-treated tubes. Peripheral blood mononuclear cells (PBMCs) were isolated on Lymphoprep™ density-gradient centrifugation according to the instructions of the manufacturer (Axix-Shield Po CAS, Oslo, Norway). Establishment of LCLs was performed in our laboratory, by infecting peripheral blood lymphocytes with the Epstein Barr virus following previous described procedures (Miller, 1982).

LCLs were cultured in suspension in RPMI 1640 medium (Cat#21875034, Gibco/Thermo Fisher, Waltham, MA, USA), 1×10^6 cells/mL supplemented with 1 % penicillin/ streptomycin (Cat#15140-122, Gibco/Thermo Fisher Waltham, MA, USA) and 10 % (v/v) fetal bovine serum (FBS) (Cat#: F7524 Merck, Madrid, Spain) in T flasks held upright at 37 °C in a humidified 5 % CO_2 atmosphere. LCLs were used individually, and experiments were not conducted in a blinded manner. For validation experiments, LCLs were treated with tideglusib (5 μM) or vehicle for 24 h previously to the RNA extraction. This dose and treatment time were previously successfully used for recovery TDP-43 homeostasis in these cells (Martínez-González et al., 2021). The GSK-3β inhibitor, tideglusib, was synthetized in our laboratory following previously described procedures (Martínez Gil et al., 2005).

2.3. NGS sample preparation

Pellets of the fifteen samples of lymphoblasts mentioned in Table 1 were summited for miR-Seq analysis to Qiagen Genomic Services (Fig. S1a). RNA was isolated from approximately 2×10^6 cells using the miRNeasy Mini Kit (QIAGEN) according to manufacturer's instructions with an elution volume of 40 μL.

2.4. Library preparation and sequencing

The library preparation was done by Qiagen Genomic Services using the QIAseq miRNA Library Kit (QIAGEN). A total of 100 ng total RNA was converted into miRNA NGS libraries. After adapter ligation, unique molecular identifiers (UMIs) were introduced in the reverse transcription step. The cDNA was amplified using PCR (16 cycles) and during the PCR indexes were added. After PCR the samples were purified. Library preparation was quality controlled using capillary electrophoresis (Tape D1000). Based on quality of the inserts and the concentration measurements, the libraries were pooled in equimolar ratios. The library pool(s) were quantified using qPCR. The library pool(s) were then sequenced on a NextSeq (Illumina Inc.) sequencing instrument according to the manufacturer instructions. Raw data was de-multiplexed and FASTQ files for each sample were generated using the bcl2fastq2 software (Illumina inc.). RNA-seq raw data have been deposited in the Gene Expression Omnibus under the accession number GSE287831 (submitter Eva P. Cuevas).

2.5. Read mapping, quality control, and quantification of gene expression

All primary analyses were carried out by Qiagen Genomic Services using CLC Genomics Server 21.0.4. Using the Qiagen platform, an

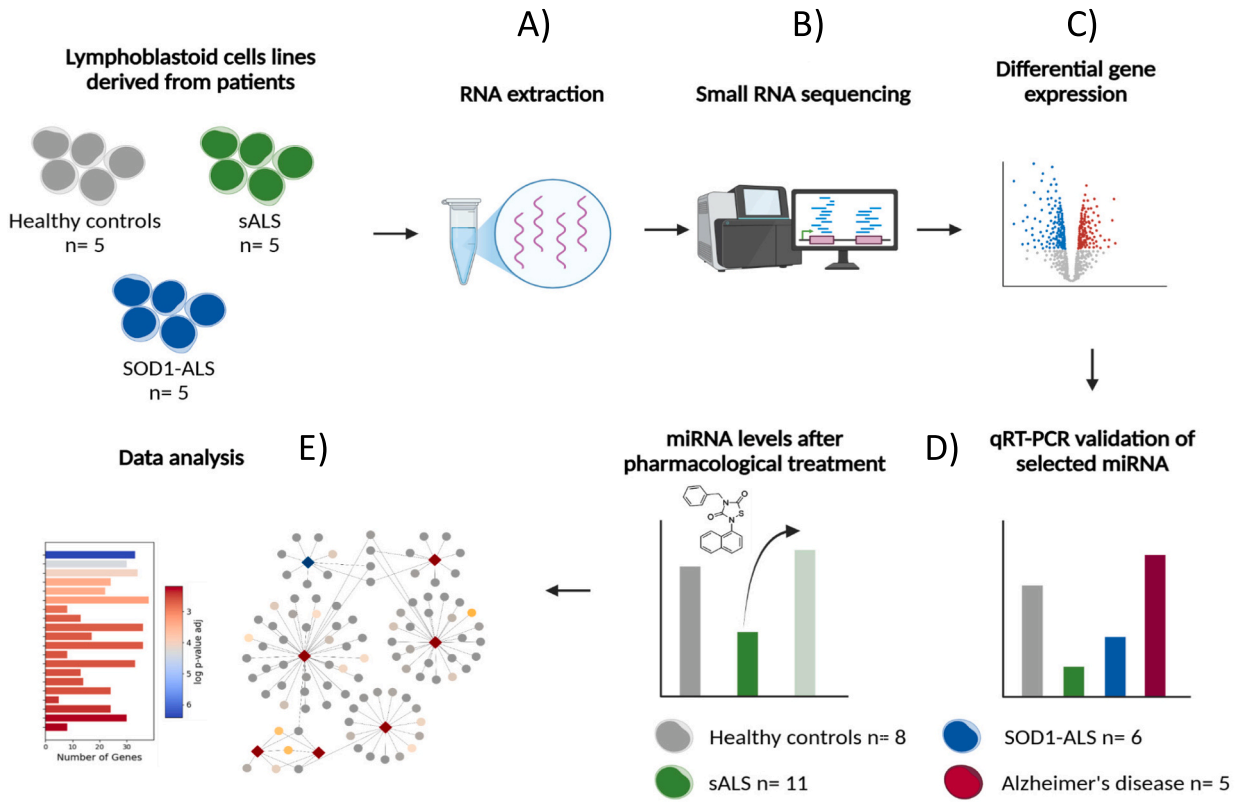

Fig. 1. Experimental design flow-chart. Type (healthy control, sALS, SOD1-ALS and Alzheimer's disease) and number (n) of lymphoblast human samples are depicted. Full description of each individual sample is collected in Table 1. Different steps using in the overall study include: A) RNA extraction from different LCLs of healthy controls, sALS and SOD1-ALS; B) small RNA sequencing; C) differential gene expression considering different comparisons between samples; D) qRT-PCR validation of the selected miRNAs and determination of miRNAs levels after pharmacological treatment; E) data analysis using systems pharmacology.

average of 21.7 million reads per sample was generated (Fig. S1b). The transcriptomic data exhibited excellent sequencing quality, with a median PHRED score of 36 across the entire read length for all samples (Fig. S1c). All the quality control metrics for each sample can be found in Zenodo (doi: https://doi.org/10.5281/zenodo.14711697).

These reads were subsequently processed and mapped to the miRNA database (miRbase) to identify the expressed miRNAs in each sample. The workflow "QIAseq miRNA Quantification" of CLC Genomics Server with standard parameters was used to map the reads. In short, the reads were processed by (1) trimming of the common sequence, UMI and adapters, and (2) filtering of reads with length < 15 nt or length > 55 nt (Fig. S1d–f). They were then deduplicated using their UMI. Reads were grouped into UMI groups when they (1) started at the same position based on the end of the read to which the UMI was ligated (i.e., Read2 for paired data), (2) were from the same strand, and (3) have identical UMIs. Groups that contained only one read (singletons) were merged into non-singleton groups if the singleton's UMI could be converted to a UMI of a non-singleton group by introducing an SNP (Figs. S1e–f). Deduplicated reads were mapped to miRBase and piRNAdb (Barreñada et al., 2021) (Figs. S2a–b). The proportion of successfully mapped reads ranged from 26 % to 51 %, with higher proportions of piRNA-mapped reads in five samples (Fig. S2c). For downstream analysis, data were filtered to retain reads between 15 and 55 nucleotides.

The 'Empirical analysis of DGE' algorithm of the CLC Genomics Workbench 21.0.4 was used for differential expression analysis with default settings. It was an implementation of the 'Exact Test' for two-group comparisons developed by Robinson and Smyth (Robinson and Smyth, 2008), and incorporated in the EdgeR Bioconductor package (Robinson et al., 2010).

For all unsupervised analysis, only miRNAs were considered with at least 10 counts summed over all samples. A variance stabilizing transformation was performed on the raw count matrix using the function variance-stabilizing transformation (VST) of the R package DESeq2 version 1.28.1. 500 genes with the highest variance were used for the Principal Component Analysis (PCA). The variance was calculated agnostically to the pre-defined groups (blind = TRUE).

2.6. Differential expression data analysis

Volcano plots were generated using Python 3.9.15 with the Pandas 1.5.2 and Matplotlib 3.6.2 libraries. For this purpose, fold change $|\log_2$ fold change$| \geq 1.5$ and p-value < 0.01 were used to identify potential dysregulated miRNAs that could be involved in ALS pathology and select miRNAs for further validation. Heatmap was designed using Seaborn 0.12.2 hierarchical clustering algorithm. The resulting code can be found in Zenodo (doi: https://doi.org/10.5281/zenodo.14711697).

2.7. miRNA validation by quantitative real-time PCR (qRT-PCR)

RNA extraction, cDNA synthesis and quantitative polymerase chain reaction (PCR) were performed using miRNeasy mini kit, miRCURY LNA RT kit and miRCURY LNA SYBR Green PCR kit (all from QIAGEN), respectively, according to manufacturer's instructions. Quantitative real-time PCR was performed with LightCycler® 96 System and the associated software using the manufacturer's recommended conditions. The miRCURY LNA miRNA PCR Assay (Qiagen) was used in qRT-PCR. The specific miRNA PCR primer sets utilized are listed in the Table 2. Each reaction was performed in biological duplicates in at least two independent experiments. Data analysis was based on the relative gene expression data using qRT-PCR and the $2^{-\Delta\Delta CT}$ method (Livak and Schmittgen, 2001). For normalization, hsa-miR-19b-3p, hsa-miR-26b-5p and hsa-let-7g-5p were selected as the optimal normalization miRNAs according to their expression stability between samples using Normfinder Software (Table 3). The arithmetic mean of the three miRNAs was used as the normalization value. UniSp6 RNA Spike-in was utilized to assess the efficacy of reverse transcription. The validation of miRNAs for qRT-PCR were done using all the samples included in Table 1 and depicted in Fig. 1.

Table 2
List of miRCURY LNA miRNA PCR assays. The grey ones correspond to those use for normalization and for assesing the efficacy of reverse transcription

miRCURY LNA miRNA PCR Assay	Reference
hsa-miR-205-5p	YP00204487
hsa-miR-3150b-3p	YP0210925
hsa-miR-3689e (3689a-5p)	YP02113857
hsa-miR-3689f	YP02106748
hsa-miR-509-3p	YP00204458
hsa-miR-513a-5p	YP00205900
hsa-miR-513b-5p	YP00205620
hsa-miR-513c-5p	YP00205928
hsa-miR-6821-5p	YP02108669
hsa-miR-19b-3p	YP00204450
hsa-let-7g-5p	YP00204565
hsa-miR-26b-5p	YP00204172
UniSp6 (339306)	YP00203954

2.8. miRNA – target network and functional enrichment analysis

To elucidate the role of the validated miRNAs in ALS pathology, miRNA – gene interactions were profiled and analyzed using network pharmacology approaches. miRTARBase database (Hsu et al., 2011) (v.9.0) was used to identify all the experimentally reported gene-interactions of our validated miRNAs. OpenTarget database (Koscielny et al., 2017) (v.23.12) was employed to consider only those genes reported to be involved in ALS disease. The Human Protein Atlas database (Thul and Lindskog, 2018) (v.23.0) was collated to discard those genes reported as not detected (nTPM <1) in lymphoid tissues. Finally, Cytoscape software (Shannon et al., 2003) (v.3.10.0) was used to assemble the miRNA – gene interaction network. Metascape (Zhou et al., 2019) was used to detect the potential molecular pathways altered in our samples. Adjusted p-value (Benjamini-Hochberg correction) was employed to ensure statistical significance. All the data analysis was carried out with KNIME Analytics Platform (Tiwari and Sekhar, 2007) (v.4.7.8), and the corresponding workflow, together with all the input data, can be found in the Zenodo repository (doi: https://doi.org/10.5281/zenodo.14711697).

2.9. Statistics

The resulting data from qRT-PCR validation were expressed as the mean ± standard error of the mean (SEM). Student's *t*-test was used to assess statistical differences when comparing only two groups, while ANOVA test followed by the Bonferroni post hoc test was used to compare three or more groups. Receiver operating curves (ROC) were drawn by plotting the sensitivity against 1 – specificity for different cutoff values. Areas under the ROC curves (AUC) were subsequently calculated. Those miRNAS with an AUC > 0.8 and a p-value < 0.05 were considered as potential biomarkers. Statistical analyses were conducted using GraphPad Prism 8.0 (San Diego, CA, USA).

3. Results

3.1. Sequencing of the small RNA fraction in lymphoblasts

The small RNA fraction sequencing was performed on fifteen samples of lymphoblasts derived from healthy controls, sporadic ALS (sALS), and familial SOD1 ALS patients (Table 1). Principal Component Analysis (PCA) of all samples (healthy controls, sALS, and SOD1-ALS)

Table 3
Data from the Normfinder analysis with the best candidate miRNAs to be reference genes in our cells. The selected reference miRNAs appear in bold (CPM: counts per million).

Name	Average CPM	Standard Deviation	Coefficient of Variation
hsa-miR-19b-3p	13174,6821	866,700961	0,065785342
hsa-let-7g-5p	13789,7054	1058,039104	0,076726737
hsa-miR-26b-5p	10800,1987	864,3911962	0,080034749
hsa-miR-15b-5p	4819,50375	401,5969143	0,083327441
hsa-let-7d-5p	2587,98323	221,3966569	0,085547949
hsa-miR-19a-3p	1961,23937	178,5827236	0,091056057
hsa-let-7f-5p	63128,4621	5841,863282	0,092539293
hsa-miR-148b-3p	1396,68588	137,3752309	0,098358001
hsa-miR-30e-5p	7696,54082	773,9438085	0,100557358
hsa-miR-374a-5p	584,988944	59,56557695	0,101823423

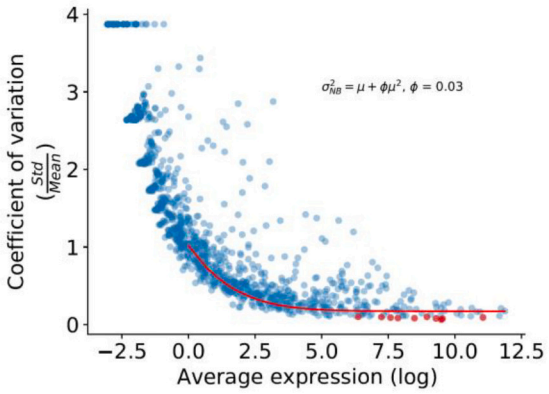

demonstrated a greater variability in sALS samples than in the other two groups (Fig. 2). This variability is consistent with the high degree of clinical heterogeneity characteristic of sALS patients (Sabatelli et al., 2013).

Data examination revealed a peak at the expected miRNA length of approximately 21 nucleotides, while five samples exhibited a secondary peak at around 30 nucleotides. This is indicative of a high proportion of piwi-interacting RNAs (piRNAs) in these samples, which are regulatory small noncoding RNAs involved in gene regulation (Wu et al., 2020).

Volcano plots are a useful way to visualize the magnitude, direction and significance of differential expression between two experimental subjects. Therefore, we generated volcano plots of piRNAs differential expression levels to identify up- or down-regulated piRNAs. Fig. 3 shows the relationship between piRNA p-values and fold changes among the samples.$|\log2 \text{ fold change}| \geq 1.5$ and p-value < 0.01. were used as criteria to identify potential up- or down-regulated piRNA. The following comparative analyses were performed: sALS vs. healthy controls, SOD1-ALS vs. healthy controls, and ALS-disease (sALS + SOD1-ALS) vs. healthy controls (Fig. 3a). Our results showed that only two piRNAs, hsa-piR-33168 and hsa-piR-33188, were down-regulated in the samples from sALS patients compared to healthy controls, which can be found in the other two proposed comparisons (Fig. 3a, b). Surprisingly, we found a large set of piRNAs with lower expression in the comparison of SOD1-ALS patients versus controls (Fig. 3a). Specifically, those exhibiting the greatest change in expression are hsa-piR-5747, hsa-piR-28,764, hsa-piR-24,541, hsa-piR-27,484, and hsa-piR-5748. In terms of potential up-regulated piRNAs, we only found hsa-piR-32,171 in the ALS disease versus healthy control comparison (Fig. 3a, b). These results suggest a distinct dysregulation of piRNAs in lymphoblasts from SOD1-ALS patients compared to sALS, providing a starting point to elucidate the underlying differences between these types of patients.

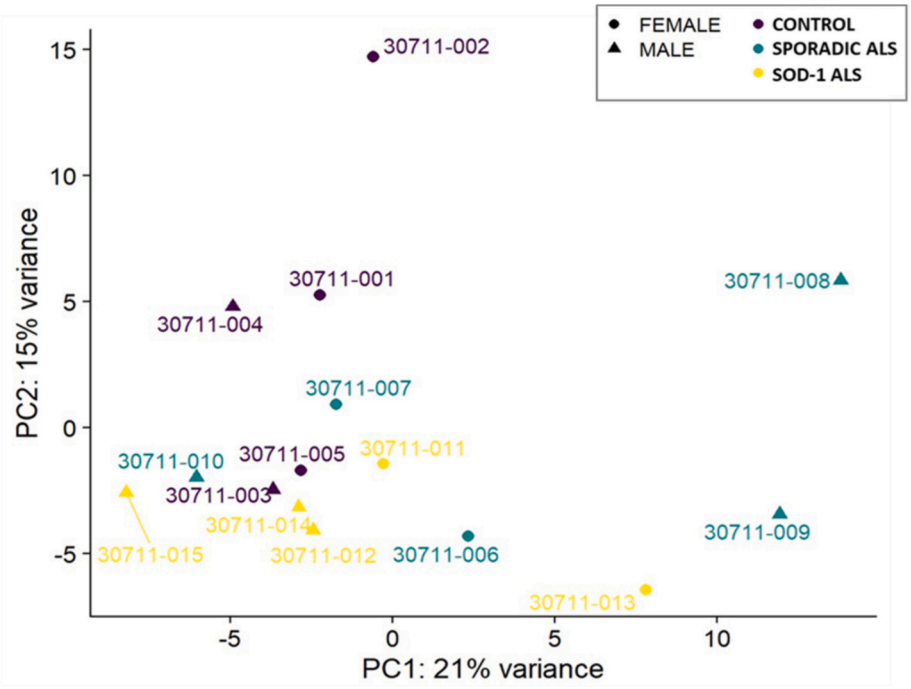

Fig. 2. Principal component analysis (PCA) of the small RNA fraction sequencing from human lymphoblasts (healthy, sALS and SOD1-ALS).

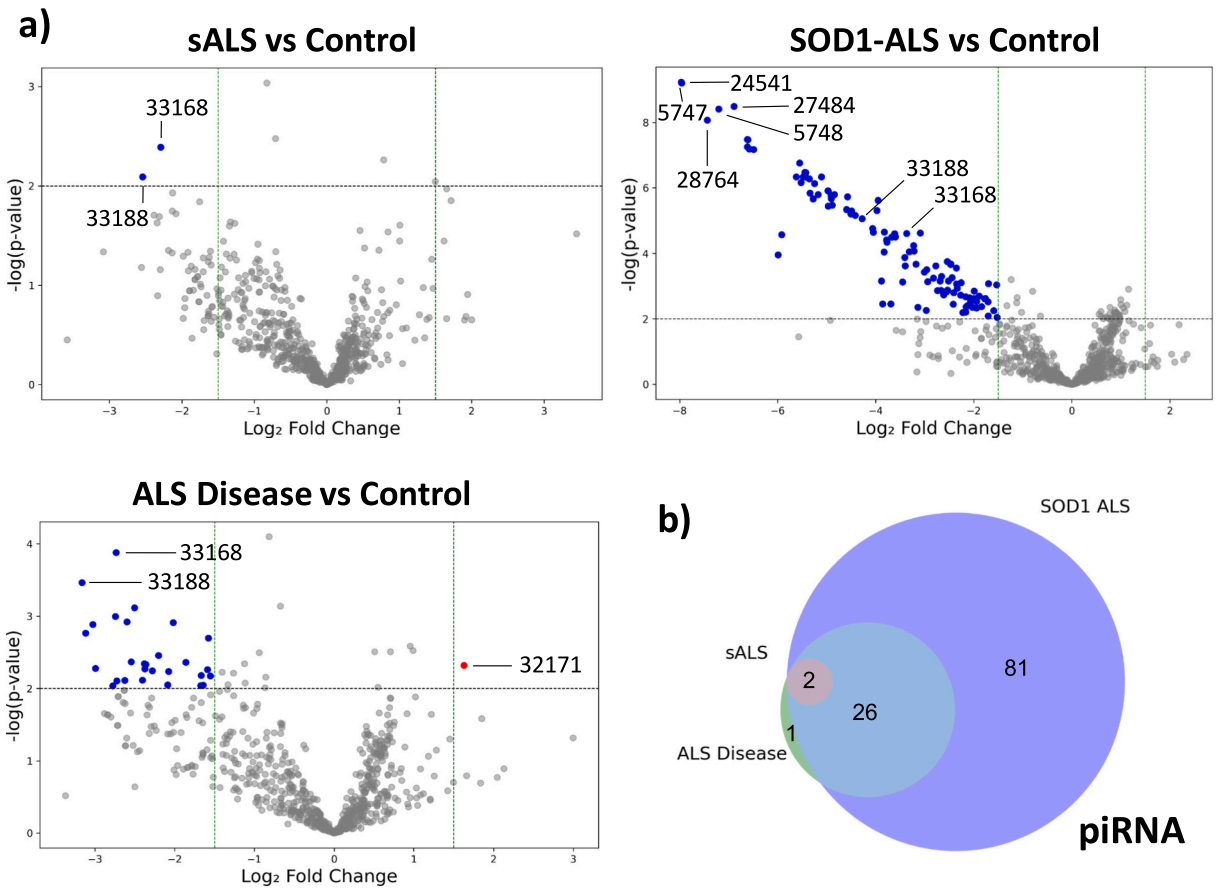

Fig. 3. a) Volcano plot representations of the differential piRNA expression for each comparison. Thresholds are defined by |log2 fold change| ≥ 1.5 and p-value < 0.01. Down-regulated and up-regulated miRNAs are marked in blue and red, respectively. b) Venn diagram representing the number of dysregulated piRNAs identified in the three comparisons. (For interpretation of the references to color in this figure legend, the reader is referred to the web version of this article.)

3.2. Analysis of differentially expressed miRNAs in lymphoblasts

Volcano plots of miRNAs differential expression levels in control versus sALS or SOD1-ALS samples were generated to identify up- or down-regulated miRNAs. As shown in Fig. 4a, the comparison between sALS and healthy controls revealed 11 dysregulated miRNAs, with 9 up-regulated and 2 down-regulated. Similarly, in the comparison between SOD1-ALS and healthy controls, 13 miRNAs were dysregulated, with 7 up-regulated and 6 down-regulated. ALS-disease versus healthy controls showed 8 up-regulated and 3 down-regulated miRNAs. When considering a p-value < 0.01, only two miRNAs were common to all comparisons: a down regulation of hsa-miR-6821-5p, and an up-regulation of hsa-miR-3150b-3p (Fig. 4b). Regardless of the p-value, hierarchical clustering of the volcano plot-selected miRNAs confirmed the existence of two sets of miRNAs. Despite the observed differences in the magnitude of fold change, 8 miRNAs are down-regulated, while 15 miRNAs tend to be up-regulated (Fig. 4c).

Due to the multiple comparisons in the experimental design, the p-value criteria often lead to an increase in the false positive rate. To avoid this, we performed a subsequent validation of the identified miRNAs conducted through qRT-PCR. We selected a group of seven miRNAs common in at least two comparisons and/or with great magnitude of expression levels (Fig. 4b). Moreover, further analysis of the data revealed two miRNAs that presented high fold change values (|$\log_2$ fold change| ≥ 1.5). However, due to their compromised p-value (p-value >0.01), these would have been excluded according to the volcano plot filtering criteria. Specifically, these were: hsa-miR-3689f common to sALS ($\log_2$ fold change = 5.875232163, p-value = 0.010922014), SOD1-ALS ($\log_2$ fold change = 5.214531178, p-value = 0.024250551), and ALS-Disease ($\log_2$ fold change = 5.58208199, p-value = 0.012278682), and hsa-miR-509-3p, present only in the sALS subset ($\log_2$ fold change = 5.229290982, p-value = 0.019568025) and in the ALS-Disease group ($\log_2$ fold change = 4.311538921, p-value = 0.054157599). Both miRNAs were also selected for qRT-PCR validation, as shown in Fig. 4. Overall, the nine miRNAs selected for final validation are summarized in Fig. 4d.

3.3. Validation of the selected dysregulated miRNA candidates in lymphoblasts

The subsequent validation was performed by qRT-PCR. The selection of optimal reference miRNAs for data normalization was achieved through the utilization of the NormFinder software, leading to the selection of hsa-miR-26b-5p, hsa-miR-19b-3p, and hsa-miR-let-7g-5p as endogenous references. Expression changes in the nine selected miRNAs (Fig. 4c) were validated using a larger cohort of lymphoblast samples: 17 ALS samples (11 sporadic and 6 SOD1) and 8 healthy controls (Table 1). Significant differences in expression were confirmed for the majority of candidate miRNAs. Up-regulation of several miRNAs, including hsa-miR-509a-3p, hsa-miR-513a-5p, hsa-miR-513c-5p, hsa-miR-3150b-3p, hsa-miR-3689a-5p, and hsa-miR-3689f, was validated in sALS patients compared to healthy controls. A similar up-regulation trend was observed for hsa-miR-205-5p and hsa-miR-513b-5p. In SOD1-ALS samples, an up-regulation trend for hsa-miR-205-5p and hsa-miR-3150b-3p was also observed compared to healthy controls, although it did not reach statistical significance (Fig. 5). Notably, hsa-miR-6821-5p was observed to be down-regulated in both sALS and SOD1-ALS, corroborating the NGS data.

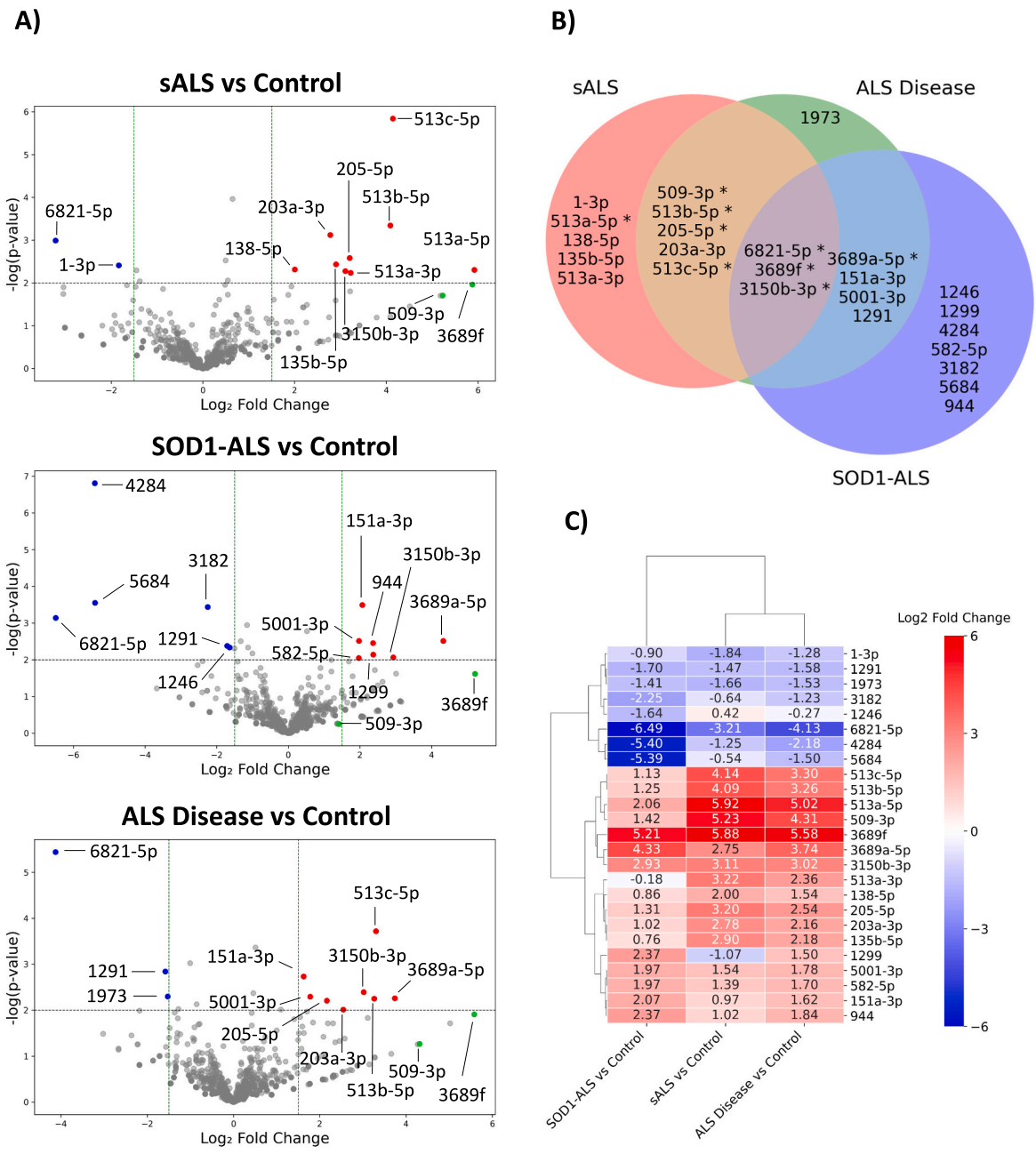

D)

hsa-miR-205-5p	hsa-miR-513b-5p	hsa-miR-3689a-5p
hsa-miR-509-3p	hsa-miR-513c-5p	hsa-miR-3689f
hsa-miR-513a-5p	hsa-miR-3150b-3p	hsa-miR-6821-5p

Fig. 4. a) Volcano plot representations of the differential miRNA expression for each comparison. Thresholds are defined by |log2 fold change| ≥ 1.5 and p-value < 0.01. Down-regulated and up-regulated miRNAs are marked in blue and red, respectively. Manually selected miRNAs are marked in green b) Venn diagram of dysregulated miRNAs in the three comparisons according the volcano plot filtering. miRNAs are indicated as their identifying code. Asterisks denote the selected miRNA for RT-qPCR validation c) Heatmap representation of the differentially expressed miRNA according to the three comparisons. d) Selected miRNAs obtained in the NGS for further validation. (For interpretation of the references to color in this figure legend, the reader is referred to the web version of this article.)

To assess the specificity of the nine selected candidate miRNAs for ALS (Fig. 4c) the expression levels of these miRNAs were tested in five LCLs derived from Alzheimer's disease (AD) patients using qRT-PCR. Among the nine candidates, five miRNAs (hsa-miR-205-5p, hsa-miR-509-3p, hsa-miR-3689a-5p, hsa-miR-3689f, and hsa-miR-6821-5p) were found to be up-regulated in AD samples compared to healthy controls (Fig. 6). An up-regulation trend for hsa-miR-213a-5p ($p = 0.07$) and hsa-miR-3150b-3p ($p = 0.08$) was also observed compared to healthy controls.

It is noteworthy that hsa-miR-6821-5p demonstrated a contrasting

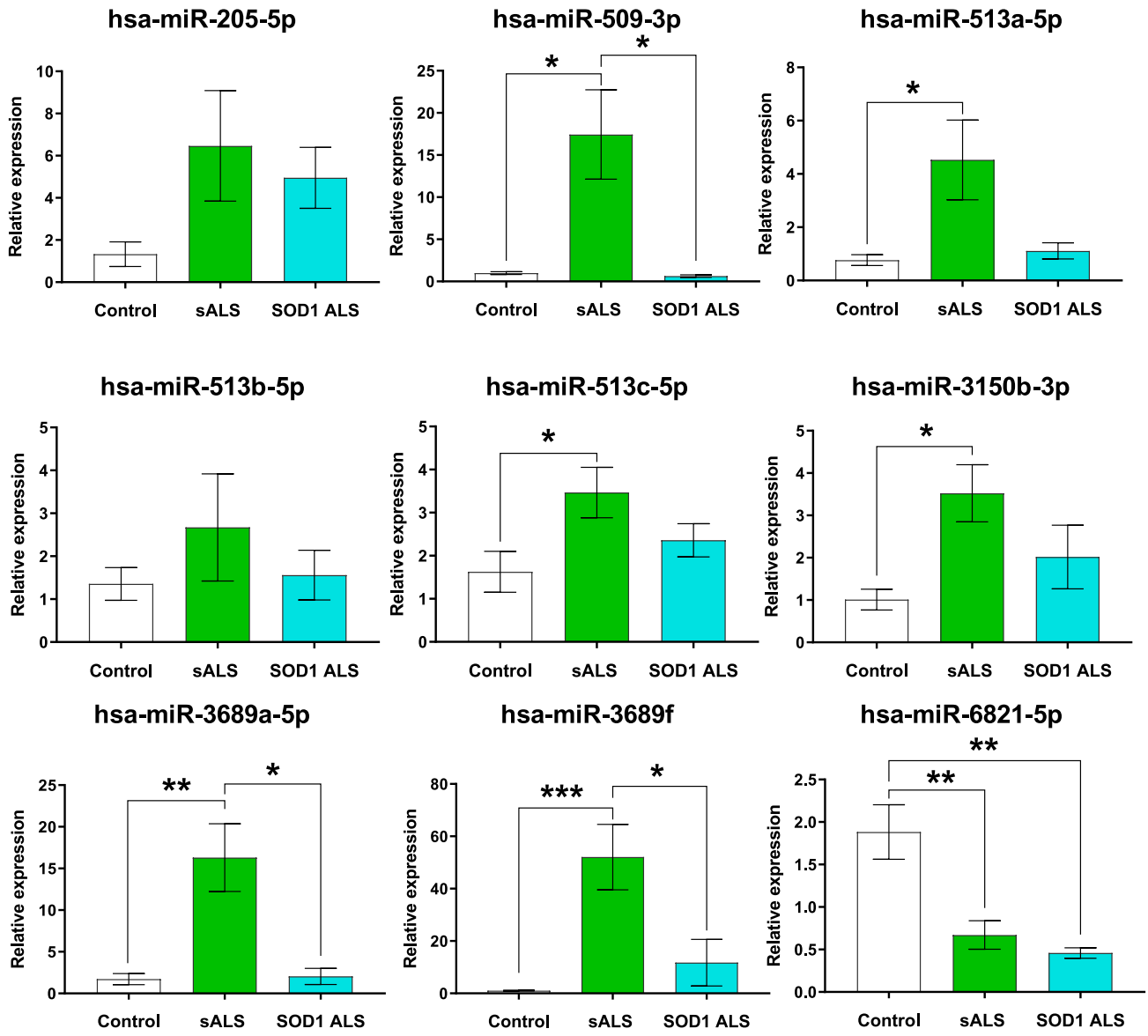

Fig. 5. Validation of miRNA expression by qRT-PCR. The relative expression levels of nine miRNAs were quantified in sALS (n = 11) and SOD1-ALS (n = 6) samples compared to the healthy controls (n = 8). The data represent the mean of at least two independent experiments performed in duplicate. Error bars denote SEMs and the ANOVA test followed by Bonferroni post hoc test was used for statistical calculations. *p < 0.05, **p < 0.01, ***p < 0.001.

behaviour, exhibiting a decrease in ALS lymphoblasts (Fig. 5) and a significant increase in AD lymphoblasts (Fig. 6) relative to healthy controls. This observation highlights the potential disease-specific dysregulation of miRNAs, thereby underscoring the clinical implications of this particular miRNA profile in differentiating between neurodegenerative diseases (Fig. S4).

3.4. Diagnostic potential of the miRNAs profile by receiver operating characteristic analysis

The diagnostic performance of our candidate miRNAs in distinguishing patients from control group was assessed by means of the receiver operating characteristic (ROC) curves and determining the area under the curve (AUC) (Mandrekar, 2010) (Fig. 7). The ROC curve analysis revealed a diagnostic potential for each of the following five miRNAs: hsa-miR-513a-5p, hsa-miR-513c-5p, hsa-miR-3150b-3p, hsa-miR-3689f and hsa-miR-6821-5p for sALS (Fig. 7, left panel). In all these cases the p-value is less than 0.05 with AUC values ranging from 0.82 to 1.00 (Fig. 7). Although p-value for hsa-miR-3689f is 1, being dysregulated in the 100 % of the studied sALS regarding the controls, its diagnostic potential should be validated in the next future using a larger number of samples.

When comparing all ALS samples (sporadic and SOD1) to healthy controls, the ROC curves revealed that only hsa-miR-3689f and hsa-miR-6821-5p have diagnostic value, with p-values < 0.01 and AUC values of 0.93 and 0.97, respectively (Fig. 7, right panel).

3.5. miRNAs profile distinguishing bulbar and spinal ALS subtypes

Recently, some efforts have been focused on identifying miRNAs as promising biomarkers in blood samples from ALS patients to differentiate between fast or slow progression of the disease (Waller et al., 2024). The samples here used offer the possibility to classify the ALS patients by the clinical presentation (bulbar or spinal subtypes), which somehow may reflect the progression time of the disease (Requardt et al., 2021).

After examination of miRNA expression levels in ALS patients with either bulbar or spinal clinical presentation, a distinct set of miRNAs

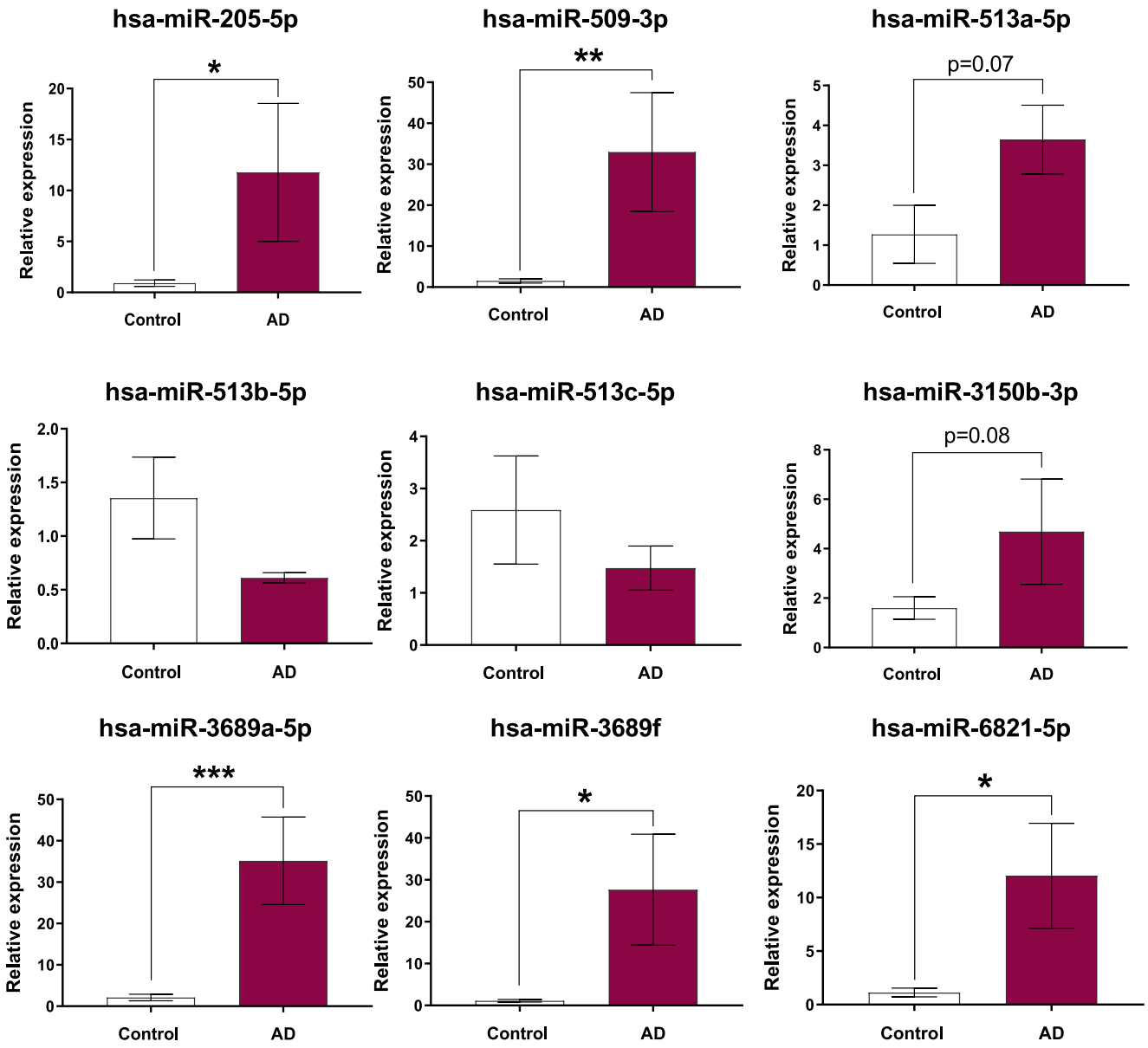

Fig. 6. miRNA expression changes in AD lymphoblast compared to the healthy controls. Five of our nine candidate miRNAs were up-regulated in AD samples. The relative expression levels of our selected miRNAs were quantified by qRT-PCR in AD samples compared to the healthy controls. The data correspond to a single experiment performed in duplicate. Error bars denote SEMs and statistical analyses were conducted using the Student's *t*-test. *p < 0.05, **p < 0.01, ***p < 0.001.

emerges as characteristic of the bulbar subtype. Up-regulation of hsa-miR-205-5p, hsa-miR-509-3p, hsa-miR-513a-5p, hsa-miR-513c-5p, hsa-miR-3150b-3p, hsa-miR-3689a-5p, and hsa-miR-6821-5p was observed in the bulbar subtype compared to healthy controls (Fig. 8). In patients with the spinal subtype, up-regulation of hsa-miR-3150b-3p and down-regulation of hsa-miR-6821-5p were observed compared to healthy controls (Fig. 8).

Those miRNAs that showed significant changes in bulbar patients also showed promising AUC values suggesting diagnostic potential (Fig. 9). On the other hand, this distribution allows us to analyze whether any of these miRNAs are able to discriminate between bulbar and spinal patients. The bulbar vs. spinal ROC curves show that the miRNAs hsa-miR-509-3p (AUC = 0.88), hsa-miR-513a-5p (AUC = 1.00) and hsa-miR-3689a-5p (AUC = 0.89), effectively differentiate between these two categories in our cohort of patients (p-value < 0.05).

3.6. The GSK-3 inhibitor tideglusib modulates miR-6821 expression

Tideglusib (TDG) is a non-ATP-competitive GSK-3 inhibitor that has demonstrated significant potential for ALS treatment (Martínez-González et al., 2021). It has been shown to restore TDP-43 homeostasis in both cellular and animal models. Given its progression through various clinical trials for dementia and its current clinical evaluation for myotonic dystrophy, tideglusib represents a strong candidate for drug repurposing in ALS therapy (NCT05105958).

To date, no data are available on the effects of tideglusib on miRNA expression in lymphoblasts from ALS patients. Given the strong down-regulation of hsa-miR-6821-5p in all ALS samples (Fig. 5) and its superior diagnostic performance (Fig. 7), we aimed to assess whether tideglusib could modulate hsa-miR-6821-5p expression, which might hold therapeutic potential. Data corresponding to the levels of the other miRNAs with the treatment are included in the supplementary file (Figs. S3 and S5). Our results reveal that upon tideglusib treatment, a significant recovery of hsa-miR-6821-5p levels in sALS samples is

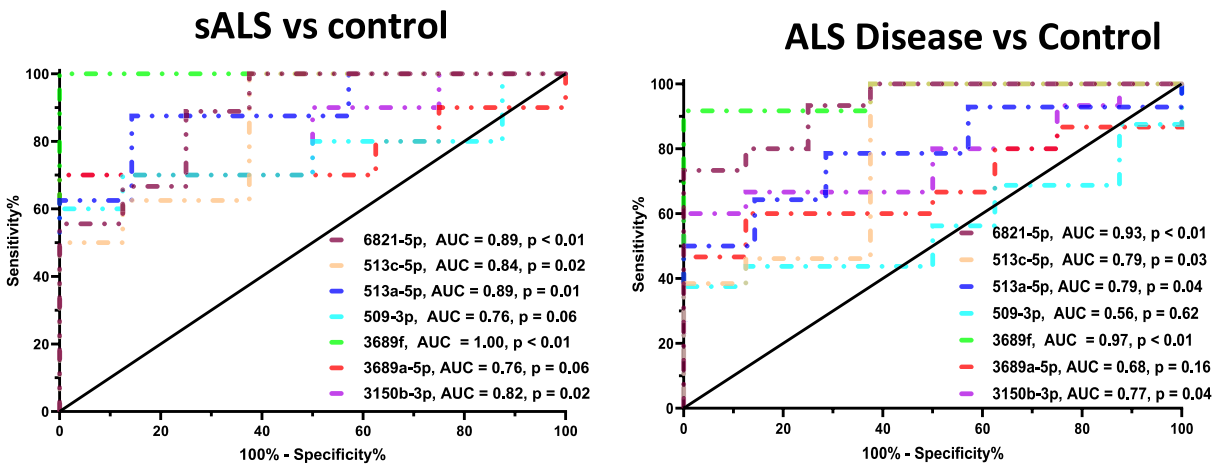

Fig. 7. Receiver operating characteristic (ROC) curves for miRNAs validated by qRT-PCR. The diagnostic performance of our candidates' miRNAs in distinguishing sALS patients from control group and ALS disease from control group was assessed by constructing receiver operating characteristic (ROC) curves and determining the area under the ROC curve (AUC) based on data from qRT-PCR.

produced, while in SOD1-ALS samples only a trend towards recovery was observed (Fig. 10). These results points to the hsa-miR-6821-5p as a potential clinical biomarker that can be determined in peripheral fluids such as lymphocytes, with diagnostic and prognostic value.

Moreover, tideglusib was able not only to rescue the expression of hsa-miR-6821-5p in the bulbar form, but also decreased the levels of hsa-miR-205-5p. These findings may suggest a specific therapeutic effect of tideglusib in fast progressive bulbar ALS patients (Fig. 11 and S5).

3.7. Functional enrichment analysis and miRNA-gene interaction network

It is well known that miRNAs exert their action by suppressing the transcription or translation of certain genes (O'Brien et al., 2018), we considered interesting to identify genes targeted by the dysregulated miRNAs found in ALS patients. This information could elucidate the involvement of these miRNAs in pathological mechanisms in ALS, in addition to discovering diagnostic potential. For this purpose, we used miRTarBase (Cui et al., 2025), a well-curated database that collects all miRNA-target interactions that have been experimentally confirmed. Our validated miRNAs were used to map gene-interaction with miRTarBase, yielding a total of 729 interactions with 646 genes. According to the methodology proposed in this work, only those genes that are expressed in lymphoid cells were considered. Therefore, the Human Protein Atlas database was used to retain only those genes that are transcribed in lymphoid tissues, resulting in 576 genes with 650 miRNA interactions. These genes were then included in an enrichment analysis to discover which molecular pathways are altered in our cohort of patients using Metascape (Zhou et al., 2019) (Fig. 12). Notably, we found that the vascular endothelial growth factor (VEGFA)/VEGF receptor system (VEGFA/VEGFR2) signaling pathway ranks first with a high statistical significance (log p_{adj}-value = −6.41), which has shown neuroprotective effects in ALS-related contexts (Vijayalakshmi et al., 2015).

To interrogate the data further, we decided to construct a miRNA-gene interaction network to search ALS-related critical genes that may be regulated by these differentially expressed miRNAs. Accordingly, the genes were filtered based on their relevance in ALS pathology using the OpenTarget database (Koscielny et al., 2017). After this filtering, a total of 108 interactions and 97 genes were displayed (Fig. 13).

Interestingly, up-regulated miRNAs showed interactions with genes closely related to ALS, such as *SIGMAR1*, *HNRNPA1* and *TARDBP*. Because miRNAs are indeed able to reduce gene expression, these interactions would indicate that *SIGMAR1*, *HNRNPA1* and *TARDBP* may be down-regulated in sALS patient samples, providing further insights into the underlying mechanisms of ALS pathogenesis.

4. Discussion

ALS is a devastating neurodegenerative disease for which there is neither effective therapy nor clinically relevant biomarkers. With an average life expectancy of 3–5 years post-diagnosis, it is critical to identify reliable biomarkers that can shorten diagnostic time, facilitate the evaluation of emerging therapies, and improve the success of clinical trials through better patient stratification. To this end, numerous recent studies have explored biomarkers in peripheral fluids, which could simplify translation to clinical practice (Irwin et al., 2024). Proteins such as neurofilaments, SOD1, and TDP-43 are under consideration, alongside cryptic exons and microRNAs (miRNAs).

miRNAs are small (20–24 nts) non-coding RNAs that regulate gene expression at the post-transcriptional level, influencing both the stability and translation of mRNAs. Increasing evidence suggests that the molecular changes associated with neurodegenerative diseases occur not only in the central nervous system but also in peripheral cells such as lymphocytes, fibroblasts, platelets, and red blood cells (Wojsiat et al., 2017). Notably, lymphoblasts from ALS patients replicate TDP-43 pathology, making them a valuable pharmacological platform for studying molecular pathology and evaluating new drug candidates (Posa et al., 2019).

Using next-generation sequencing (NGS) technology adapted to the small RNA fraction, we have characterized the miRNA signature of lymphoblasts derived from ALS patients (both sporadic and with SOD1 mutations) and healthy controls. The primary goal of this work is to identify novel diagnostic biomarkers that can be easily translated into clinical applications.

In the present study, we first noticed a significant proportion of piRNAs in addition to the miRNA peak. Intriguingly, a large number of piRNAs (>100) are down-regulated in SOD1-ALS samples compared to healthy controls, while only two piRNAs (hsa-piR-33168 and hsa-piR-33188) are differentially expressed in sALS compared to healthy controls. These results suggest a distinct role of piRNAs in lymphoblasts from SOD1-ALS patients compared to sALS, providing a starting point to elucidate the underlying differences between these two groups of patients. Although little research has been done until the moment to check the piRNAs potential role in ALS and other pathologies, the presence of piRNAs on the pyramidal tract of the medulla oblongata of sALS patients have been recently reported (Abdelhamid et al., 2022).

The analysis of miRNAs expression levels by NGS and qRT-PCR validation revealed a similar number of dysregulated miRNAs in sALS and SOD1-ALS related to control samples. However, the direction and magnitude of the fold changes differ between the two conditions. In

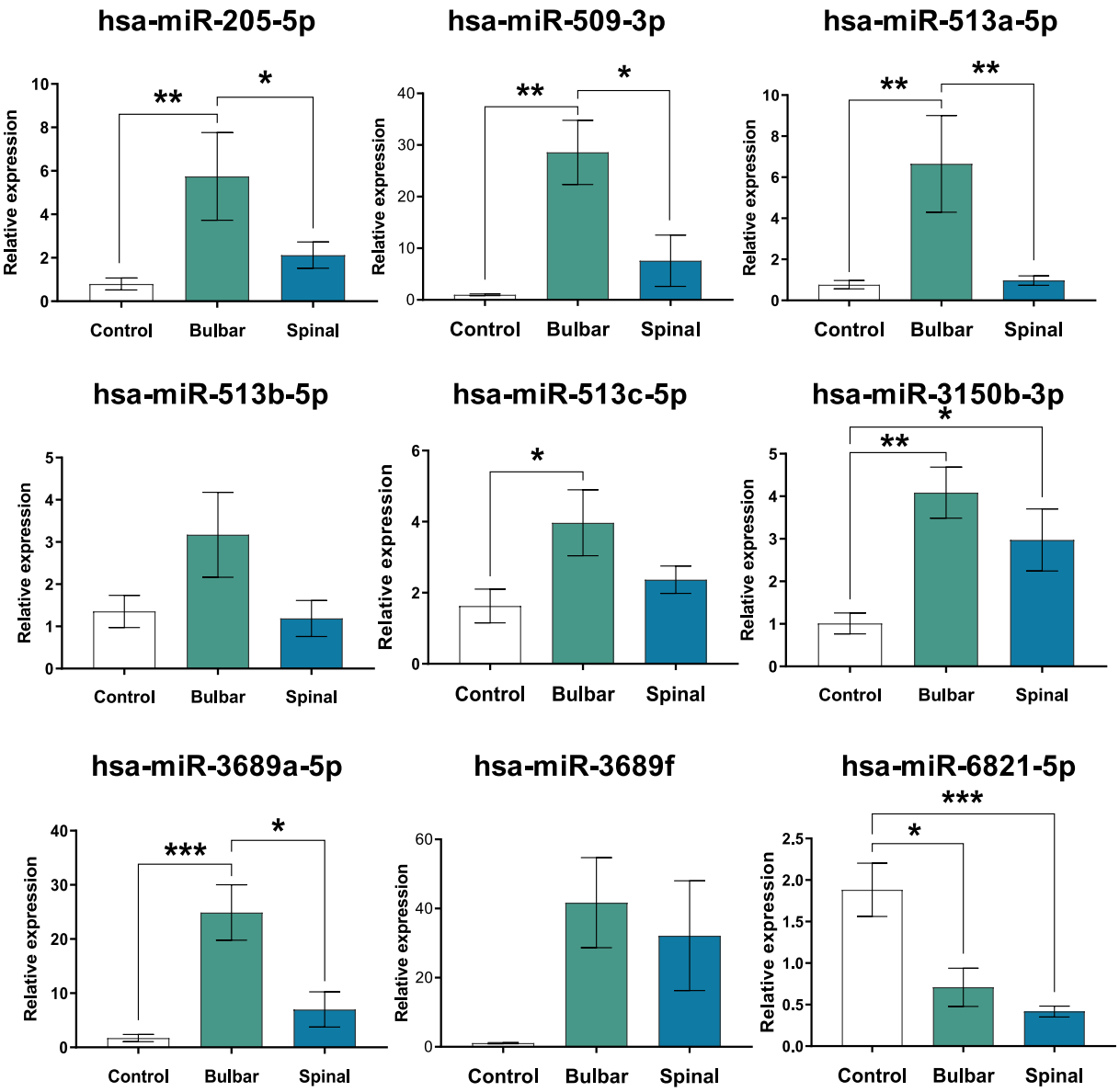

Fig. 8. miRNA Expression changes across Bulbar and Spinal ALS subtypes compared to the healthy controls by qRT-PCR. The data are the mean of at least two independent experiments performed in duplicate. Error bars denote SEMs and the ANOVA test followed by Bonferroni post hoc test was used for statistical calculations. *$p < 0.05$, **$p < 0.01$, ***$p < 0.001$.

sALS, a greater number of miRNAs are found to be up-regulated than down-regulated, in contrast to SOD1-ALS samples. After qRT-PCR validation, we then detected several miRNAs dysregulated in our ALS samples. These miRNAs, including hsa-miR-509-3p, hsa-miR-513a-5p, hsa-miR-513c-5p, hsa-miR-3150b-3p, hsa-miR-3689f, and hsa-miR-6821-5p, were altered in sALS patients relative to healthy controls, and demonstrated to have a diagnostic potential by ROC curves analyses. When comparing all ALS patients (sporadic and familial) to controls, only hsa-miR-3689f and hsa-miR-6821-5p demonstrated diagnostic utility, with p-values <0.01 and AUC values of 0.93 and 0.97, respectively. These two miRNAs need to be validated in a larger cohort of ALS patients in future studies.

There is a growing interest in identifying biomarkers capable of distinguishing faster ALS progressors to optimize clinical trials by enriching them with patients more likely to exhibit treatment effects within a limited timeframe (Din Abdul Jabbar et al., 2024). For this reason, we further analyze the miRNAs expression levels in ALS patients with either spinal or bulbar clinical presentation, the principal ALS subtypes, characterized by muscle weakness and atrophy in the limbs, or affecting speech and swallowing musculature, respectively (Masrori and Van Damme, 2020). Bulbar ALS is considered the most devastating type of the disease based on its fastest decline, the short survival, and a significantly reduced quality of life (Shellikeri et al., 2017).Here we report that several miRNAs (hsa-miR-205-5p, hsa-miR-509-3p, hsa-miR-513a-5p, hsa-miR-513c-5p, hsa-miR-3150b-3p, hsa-miR-3689a-5p, and hsa-miR-6821-5p) displayed significant changes on bulbar-onset (faster-progressing) patients relative to changes observed in samples from spinal onset ALS patients. These miRNAs also demonstrated promising diagnostic potential based on high AUC values.

Remarkably, hsa-miR-6821-5p was found to be up-regulated in AD patients but down-regulated in ALS patients, including both sporadic and SOD1 cases. This differential expression highlights its potential as ALS disease-specific biomarker. Nevertheless, further data in larger cohorts is needed to confirm these results.

As far as we know, there is not previous evidence linking these miRNAs to ALS. Notably, hsa-miR-3689f has been previously identified in B cells from various lymphomas (Jima et al., 2010), while elevated levels of hsa-miR-6821-5p have recently been associated with

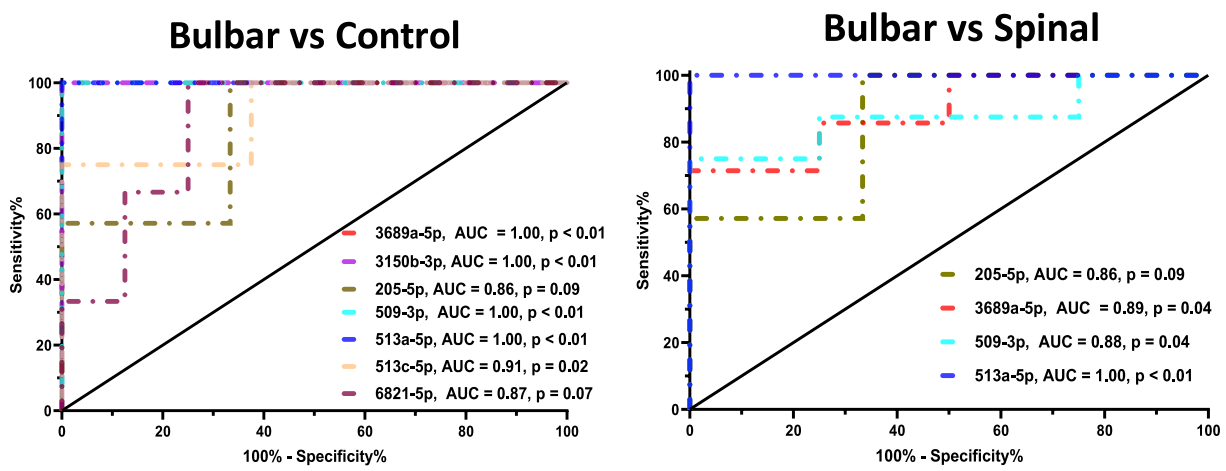

Fig. 9. Receiver operating characteristic (ROC) curves and area under the curve (AUC) based on data from qRT-PCRs showing the diagnostic performance of the set of miRNAs candidates in distinguishing bulbar versus spinal ALS onset in patients.

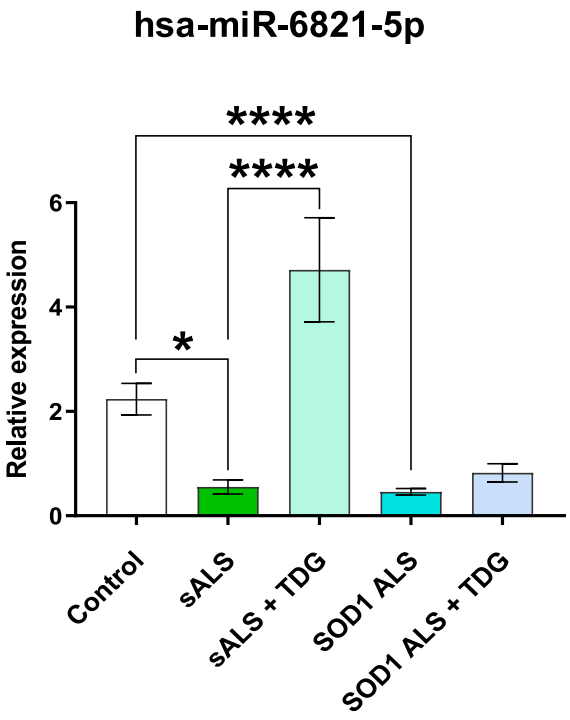

Fig. 10. hsa-miR-6821-5p levels in lymphoblasts upon tideglusib treatment by qRT-PCR. sALS and SOD1-ALS cells were treated with tideglusib (5 μM) or vehicle for 24 h previously to the RNA extraction. The data are the mean of two independent experiments performed in duplicate. Error bars denote SEMs and the ANOVA test followed by Bonferroni post hoc test was used for statistical calculations. *$p < 0.05$, ****$p < 0.0001$.

hypercholesterolemia (Escate et al., 2024).In this regard, it is noteworthy that ALS involves cholesterol dysregulation across various tissues, including muscle (Hartmann et al., 2022; Sapaly et al., 2024). Furthermore, we recently reported that lymphoblasts derived from sALS, SOD1-ALS, and c9orf72-ALS patients exhibit reduced cholesterol uptake compared to lymphoblasts from healthy controls (Etxebeste-Mitxeltorena et al., 2025). These findings align with the reduced levels of miR-6821-5p observed in lymphoblasts from ALS patients in this study. Conversely, high cholesterol levels are strongly correlated with the severity of AD (Ahmed et al., 2024). This relationship could explain the overexpression of miR-6821-5p in AD samples, and highlights the distinct roles this miRNA may play in ALS and AD.

Notably, treatment with tideglusib, a GSK-3 inhibitor currently being considered for ALS drug repurposing (Martínez-González et al., 2021), was found to rescue miR-6821-5p dysregulation in sALS samples. These results suggest that miR-6821-5p holds promise as a reliable biomarker for ALS diagnosis and prognosis, as well as a potential target for therapeutic intervention. Interestingly, treatment with tideglusib not only restored the expression of hsa-miR-6821-5p in bulbar-onset ALS samples but also decreased the levels of hsa-miR-205-5p. Remarkably, a study reported miR-205-5p regulates the apoptotic PI3K/AKT/GSK-3 signaling pathway, and reduced levels of miR-205-5p can inhibit cell invasion and transformation (Zhang et al., 2019). Many studies have shown that PI3K/AKT pathway can be activated to increase anti-apoptotic protein expression levels to improve cell survival rate and mitochondrial function in ALS. Thus, high levels of miR-205-5p may be associated to a decreased activity of PI3K/AKT/GSK-3 signaling which enhance apoptosis and GSK-3 activity resulting in cell death. This is more relevant in the aggressive bulbar ALS subtype. Intriguingly, this is in agreement with the reduction of miR205-5p levels by tideglusib and with the increased activity of GSK-3 previously found in sALS lymphoblasts (Martínez-González et al., 2021). These findings may suggest a specific therapeutic effect of tideglusib in fast progressive bulbar ALS patients.

Finally, by target prediction and enrichment analysis, we identified potential cellular pathways that may be post-transcriptional regulated by our set of miRNAs, highlighting the VEGFA/VEGFR2 system. This pathway is crucial in angiogenesis activation by inducing the proliferation, survival, sprouting and migration of endothelial cells, and also by increasing endothelial permeability (Claesson-Welsh and Welsh, 2013). Studies reported inhibition of this pathway increase the loss of lower motoneurons and axons in a model of multiple sclerosis (Stanojlovic et al., 2016) while VEGFA/VEGFR2 activity has shown neuroprotective effects in the NSC-34 motor neuron cell line (Vijayalakshmi et al., 2015). All these data may point to the therapeutic role for the VEGFA/VEGFR2 system in ALS.

Furthermore, our analysis shows that the set of miRNAs here identified may reduce *SIGMAR1*, *HNRNPA1* and *TARDBP* expression in sALS patient samples. In fact, it is well-known that the absence or down-regulation of sigma 1 receptor leads to an increase in cytosolic calcium concentration (Prause et al., 2013) being involved in several of the alterations that occur in ALS pathophysiology (Herrando-Grabulosa et al., 2021), such as the dissociation of mitochondria-ER membrane components (Watanabe et al., 2016). Similarly, reduced levels of HNRNPA1, a ribonucleo-protein responsible for the transport and metabolism of several mRNAs, have been reported in the human spinal cord of ALS patients (Honda et al., 2015). Finally, *TARDBP* codes the

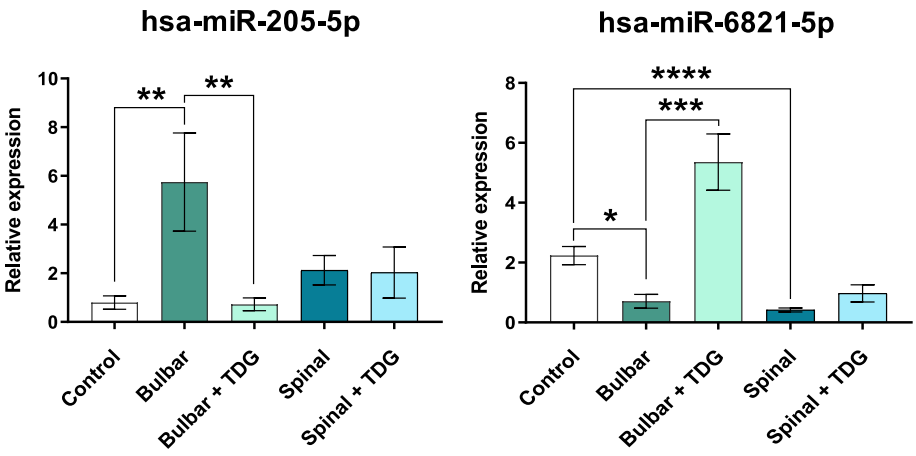

Fig. 11. Expression levels of hsa-miR-205-5p and hsa-miR-6821-5p classifying patients' cells depending on the bulbar or spinal onset and compared to the healthy controls by qRT-PCR. The cells were treated with tideglusib (5 μM) or vehicle for 24 h previously to the RNA extraction. The data are the mean of at least two independent experiments performed in duplicate. Error bars denote SEMs and the ANOVA test followed by Bonferroni post hoc test was used for statistical calculations. *p < 0.05, **p < 0.01, ***p < 0.001, ****p < 0.0001.

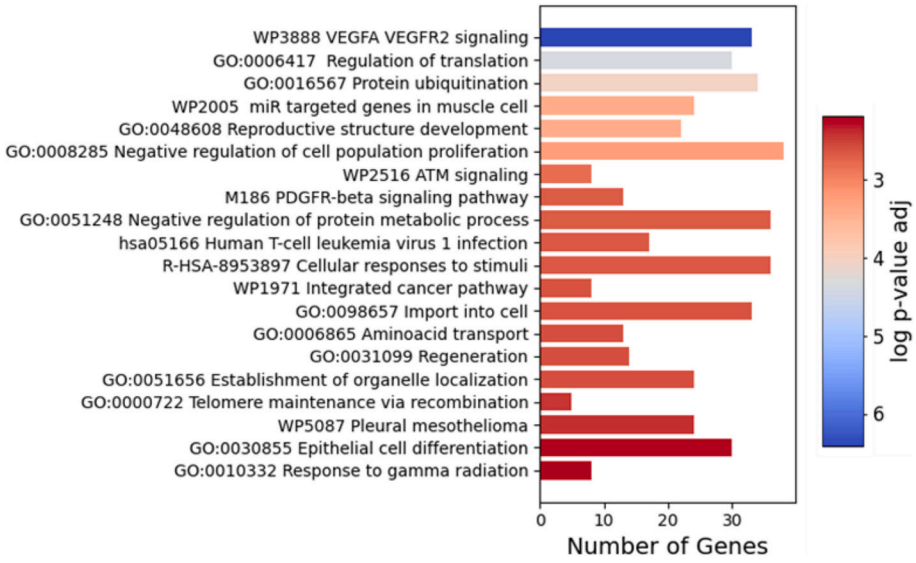

Fig. 12. Metascape enrichment analysis. Top-20 significantly enriched terms (p_{adj} -value <0.05) along with the number of genes involved.

nuclear protein TDP-43, one of the most studied protein in ALS. Our prediction suggests that hsa-miR-513a-5p could target TDP-43. Further experimentation is needed to confirm this miRNA-target relationship and its role in ALS-related contexts. Until the moment, hsa-miR513a-5p was only known to be responsible of decreased levels of progesterone receptor being a risk factor for breast cancer (Muti et al., 2018).

Altogether, our results suggest that the analysis of miRNA expression levels in lymphoblasts derived from ALS patients, offers the possibility to find potential specific biomarkers for this disease, able to discriminate between sporadic or familial ALS cases and even between clinical (spinal or bulbar) ALS presentation. The present study highlights the role of miR-6821-5p as a reliable biomarker for ALS diagnosis and prognosis, as well as a potential target for therapeutic intervention.

The current study has, however, some limitations. First at all, only one sample per patient, taking at the time of enrollment, was tested. Thus, the expression profile of miRNAs during disease progression needs to be performed. Second, our results need to be validated in larger and independent cohorts. The role of hsa-miR-6821-5p as specific role for ALS needs to be evaluated in a larger number of AD patients and other neurodegenerative diseases. It would be also important to test whether the dysregulated miRNAs, herein described, can also be observed in plasmas to easy the performance in already existing clinical infrastructures for analyses of blood. On the other hand, work aimed at detecting differential expression of these miRNAs in motor neurons from ALS patients should be done.

5. Conclusions

miRNAs hold great promise for improving ALS diagnostics, prognostics, and therapy monitoring. Their clinical use may potentially accelerate the development of personalized treatment strategies. Following this idea, we have provided a set of altered miRNAs identified in lymphoblasts from ALS patients, both sporadic and with SOD1 mutations, that may aide to the diagnostic and prognostic of ALS. Most importantly, our study showed that hsa-miR-6821-5p is down-regulated in ALS patients and demonstrates superior diagnostic potential. The further role of hsa-miR-6821-5p needs to be explored. Combining miRNA data with protein, metabolic, or imaging biomarkers could enhance diagnostic accuracy and patient stratification. The GSK-3 inhibitor tideglusib is able to rescue the expression of some of these

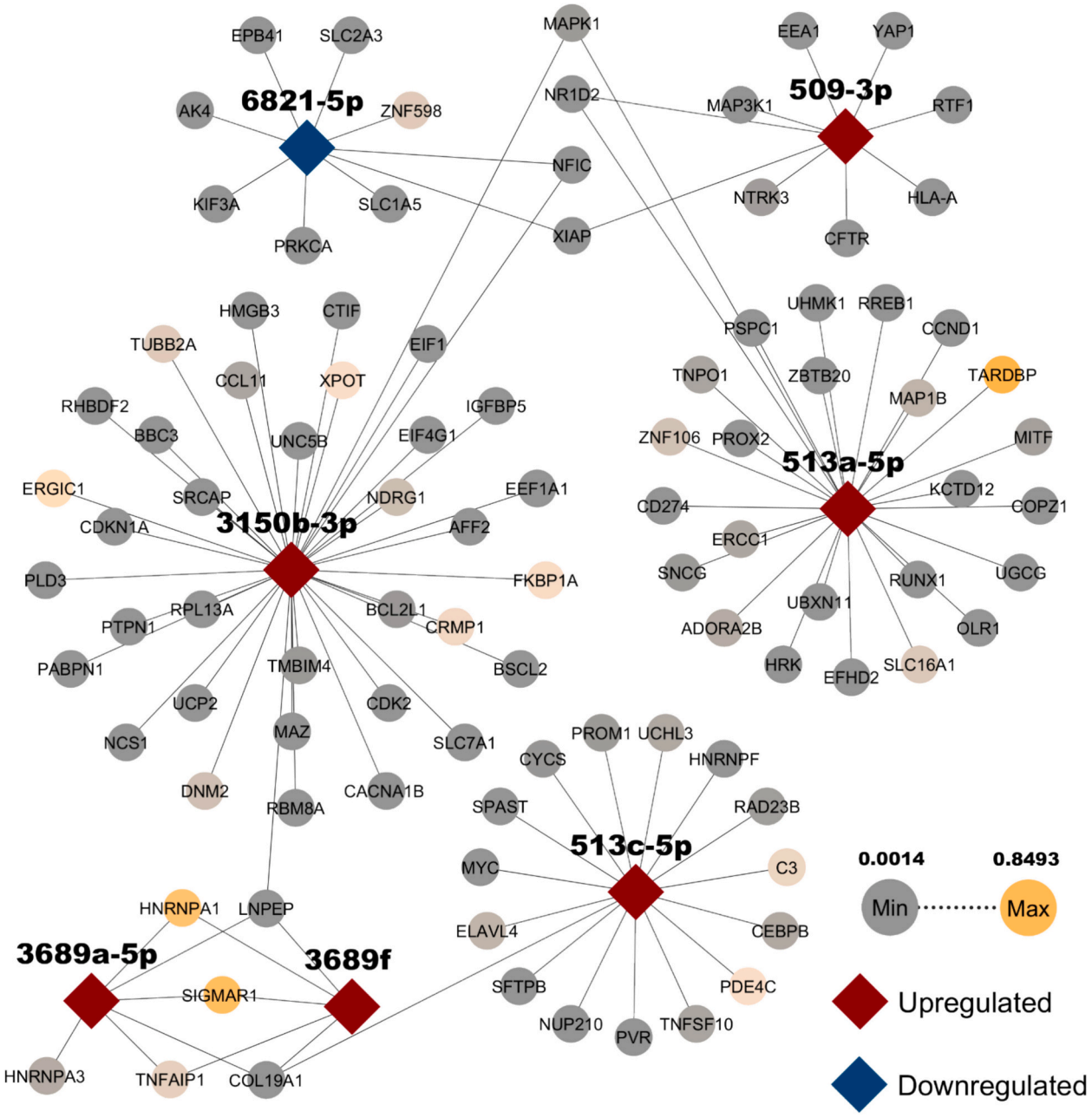

Fig. 13. miRNA-gene interaction network. The miRNAs are represented as diamonds. Up-regulated miRNAs are marked in red, whereas down-regulated miRNA is in blue. The genes, represented as circles, are colored according to the score obtained in the OpenTarget database.

miRNAs which show not only the therapeutic potential of this drug but also confirm the potential use of these biomarkers to follow the efficacy of this drug in a future clinical trial. Only large cohort and multi-center studies will confirm the utility of these miRNAs as ALS biomarkers.

CRediT authorship contribution statement

Eva P. Cuevas: Writing – review & editing, Writing – original draft, Validation, Methodology, Investigation, Formal analysis, Data curation. **Enrique Madruga:** Writing – review & editing, Writing – original draft, Visualization, Methodology, Investigation, Formal analysis, Data curation. **Ignacio Valenzuela-Martínez:** Writing – review & editing, Visualization, Investigation, Formal analysis. **David Ramírez:** Writing – review & editing, Supervision, Methodology, Formal analysis. **Carmen Gil:** Writing – review & editing, Supervision, Funding acquisition. **Siranjeevi Nagaraj:** Writing – review & editing, Formal analysis. **Angeles Martin-Requero:** Writing – review & editing, Methodology, Conceptualization. **Ana Martinez:** Writing – review & editing, Writing – original draft, Supervision, Methodology, Funding acquisition, Formal analysis, Conceptualization.

Funding

This work was supported by La Caixa and Luzón Foundation [grant number HR21-00931], and the Spanish Health Institute Carlos III [CIBERNED, grant number CB18/05/00040]. S. N. is funded with a postdoctoral fellowship from the FNRS, Belgium. E.M. is funded by MCIU (grant FPU20/03743).

Declaration of competing interest

The authors declare that they have no known competing financial

interests or personal relationships that could have appeared to influence the work reported in this paper.

Appendix A. Supplementary data

Supplementary data to this article can be found online at https://doi.org/10.1016/j.nbd.2025.106871.

Data availability

The data presented in this study are available on doi: https://doi.org/10.5281/zenodo.14711697.

References

Abdelhamid, R.F., Ogawa, K., Beck, G., Ikenaka, K., Takeuchi, E., Yasumizu, Y., Jinno, J., Kimura, Y., Baba, K., Nagai, Y., Okada, Y., Saito, Y., Murayama, S., Mochizuki, H., Nagano, S., 2022. piRNA/PIWI protein complex as a potential biomarker in sporadic amyotrophic lateral sclerosis. Mol. Neurobiol. 59 (3), 1693–1705. https://doi.org/10.1007/s12035-021-02686-2.

Ahmed, H., Wang, Y., Griffiths, W.J., Levey, A.I., Pikuleva, I., Liang, S.H., Haider, A., 2024. Brain cholesterol and Alzheimer's disease: challenges and opportunities in probe and drug development. Brain 147 (5), 1622–1635. https://doi.org/10.1093/brain/awae028.

Banack, S.A., Dunlop, R.A., Mehta, P., Mitsumoto, H., Wood, S.P., Han, M., Cox, P.A., 2024. A microRNA diagnostic biomarker for amyotrophic lateral sclerosis. Brain Commun. 6 (5), fcae268. https://doi.org/10.1093/braincomms/fcae268.

Barreñada, O., Larriba, E., Brieño-Enriquez, M.A., Del Mazo, J., 2021. piRNA-IPdb: a PIWI-bound piRNAs database to mining NGS sncRNA data and beyond. BMC Genomics 22 (1), 765. https://doi.org/10.1186/s12864-021-08071-6.

Cheng, J., Ho, W.-K., Wu, B.-T., Liu, H.-P., Lin, W.-Y., 2023. miRNA profiling as a complementary diagnostic tool for amyotrophic lateral sclerosis. Sci. Rep. 13 (1), 13805. https://doi.org/10.1038/s41598-023-40879-y.

Claesson-Welsh, L., Welsh, M., 2013. VEGFA and tumour angiogenesis. J. Intern. Med. 273 (2), 114–127. https://doi.org/10.1111/joim.12019.

Cui, S., Yu, S., Huang, H.-Y., Lin, Y.-C.-D., Huang, Y., Zhang, B., Xiao, J., Zuo, H., Wang, J., Li, Z., Li, G., Ma, J., Chen, B., Zhang, H., Fu, J., Wang, L., Huang, H.-D., 2025. miRTarBase 2025: updates to the collection of experimentally validated microRNA-target interactions. Nucleic Acids Res. 53 (D1), D147–D156. https://doi.org/10.1093/nar/gkae1072.

D'Agostino, N., Li, W., Wang, D., 2022. High-throughput transcriptomics. Sci. Rep. 12 (1), 20313. https://doi.org/10.1038/s41598-022-23985-1.

Din Abdul Jabbar, M.A., Guo, L., Nag, S., Guo, Y., Simmons, Z., Pioro, E.P., Ramasamy, S., Yeo, C.J.J., 2024. Predicting amyotrophic lateral sclerosis (ALS) progression with machine learning. Amyotroph. Lateral Scler. Frontotemporal Degener. 25 (3–4), 242–255. https://doi.org/10.1080/21678421.2023.2285443.

Escate, R., Padró, T., Pérez de Isla, L., Fuentes, F., Alonso, R., Mata, P., Badimon, L., 2024. Circulating miR-6821-5p levels and coronary calcification in asymptomatic familial hypercholesterolemia patients. Atherosclerosis 392, 117502. https://doi.org/10.1016/j.atherosclerosis.2024.117502.

Etxebeste-Mitxeltorena, M., Flores-Romero, H., Ramos-Inza, S., Masiá, E., Nenchova, M., Montesinos, J., Martinez-Gonzalez, L., Porras, G., Orzáez, M., Vicent, M.J., Gil, C., Area-Gomez, E., Garcia-Saez, A.J., Martinez, A., 2025. Modulation of mitochondria-endoplasmic reticulum contacts (MERCs) by small molecules as a new strategy for restoring lipid metabolism in an amyotrophic lateral sclerosis model. J. Med. Chem. https://doi.org/10.1021/acs.jmedchem.4c01368.

Feldman, E.L., Goutman, S.A., Petri, S., Mazzini, L., Savelieff, M.G., Shaw, P.J., Sobue, G., 2022. Amyotrophic lateral sclerosis. Lancet 400 (10360), 1363–1380. https://doi.org/10.1016/S0140-6736(22)01272-7.

Hartmann, H., Ho, W.Y., Chang, J.-C., Ling, S.-C., 2022. Cholesterol dyshomeostasis in amyotrophic lateral sclerosis: cause, consequence, or epiphenomenon? FEBS J. 289 (24), 7688–7709. https://doi.org/10.1111/febs.16175.

Herrando-Grabulosa, M., Gaja-Capdevila, N., Vela, J.M., Navarro, X., 2021. Sigma 1 receptor as a therapeutic target for amyotrophic lateral sclerosis. Br. J. Pharmacol. 178 (6), 1336–1352. https://doi.org/10.1111/bph.15224.

Honda, H., Hamasaki, H., Wakamiya, T., Koyama, S., Suzuki, S.O., Fujii, N., Iwaki, T., 2015. Loss of hnRNPA1 in ALS spinal cord motor neurons with TDP-43-positive inclusions. Neuropathology 35 (1), 37–43. https://doi.org/10.1111/neup.12153.

Horrigan, J., Gomes, T.B., Snape, M., Nikolenko, N., McMorn, A., Evans, S., Yaroshinsky, A., Della Pasqua, O., Oosterholt, S., Lochmüller, H., 2020. A phase 2 study of AMO-02 (Tideglusib) in congenital and childhood-onset myotonic dystrophy type 1 (DM1). Pediatr. Neurol. 112, 84–93. https://doi.org/10.1016/j.pediatrneurol.2020.08.001.

Hsu, S.-D., Lin, F.-M., Wu, W.-Y., Liang, C., Huang, W.-C., Chan, W.-L., Tsai, W.-T., Chen, G.-Z., Lee, C.-J., Chiu, C.-M., Chien, C.-H., Wu, M.-C., Huang, C.-Y., Tsou, A.-P., Huang, H.-D., 2011. miRTarBase: a database curates experimentally validated microRNA-target interactions. Nucleic Acids Res. 39(Database issue), D163-9. https://doi.org/10.1093/nar/gkq1107.

Irwin, K.E., Sheth, U., Wong, P.C., Gendron, T.F., 2024. Fluid biomarkers for amyotrophic lateral sclerosis: a review. Mol. Neurodegener. 19 (1), 9. https://doi.org/10.1186/s13024-023-00685-6.

Jima, D.D., Zhang, J., Jacobs, C., Richards, K.L., Dunphy, C.H., Choi, W.W.L., Au, W.Y., Srivastava, G., Czader, M.B., Rizzieri, D.A., Lagoo, A.S., Lugar, P.L., Mann, K.P., Flowers, C.R., Bernal-Mizrachi, L., Naresh, K.N., Evens, A.M., Gordon, L.I., Luftig, M., Dave, S.S., 2010. Deep sequencing of the small RNA transcriptome of normal and malignant human B cells identifies hundreds of novel microRNAs. Blood 116 (23), e118–e127. https://doi.org/10.1182/blood-2010-05-285403.

Koscielny, G., An, P., Carvalho-Silva, D., Cham, J.A., Fumis, L., Gasparyan, R., Hasan, S., Karamanis, N., Maguire, M., Papa, E., Pierleoni, A., Pignatelli, M., Platt, T., Rowland, F., Wankar, P., Bento, A.P., Burdett, T., Fabregat, A., Forbes, S., Dunham, I., 2017. Open Targets: a platform for therapeutic target identification and validation. Nucleic Acids Res. 45 (D1), D985–D994. https://doi.org/10.1093/nar/gkw1055.

Lastres-Becker, I., Porras, G., Arribas-Blázquez, M., Maestro, I., Borrego-Hernández, D., Boya, P., Cerdán, S., García-Redondo, A., Martínez, A., Martin-Requero, Á., 2021. Molecular alterations in sporadic and SOD1-ALS immortalized lymphocytes: towards a personalized therapy. Int. J. Mol. Sci. 22 (6). https://doi.org/10.3390/ijms22063007.

Li, S., Lei, Z., Sun, T., 2023. The role of microRNAs in neurodegenerative diseases: a review. Cell Biol. Toxicol. 39 (1), 53–83. https://doi.org/10.1007/s10565-022-09761-x.

Livak, K.J., Schmittgen, T.D., 2001. Analysis of relative gene expression data using real-time quantitative PCR and the 2(-Delta Delta C(T)) method. Methods (San Diego, Calif.) 25 (4), 402–408. https://doi.org/10.1006/meth.2001.1262.

Londin, E.R., Keller, M.A., D'Andrea, M.R., Delgrosso, K., Ertel, A., Surrey, S., Fortina, P., 2011. Whole-exome sequencing of DNA from peripheral blood mononuclear cells (PBMC) and EBV-transformed lymphocytes from the same donor. BMC Genomics 12, 464. https://doi.org/10.1186/1471-2164-12-464.

Ludolph, A., Drory, V., Hardiman, O., Nakano, I., Ravits, J., Robberecht, W., Shefner, J., 2015. A revision of the El Escorial criteria - 2015. Amyotroph. Lateral Scler. Frontotemporal Degener. 16 (5–6), 291–292. https://doi.org/10.3109/21678421.2015.1049183.

Lynch, K., 2023. Pathogenesis and presentation of ALS: examining reasons for delayed diagnosis and identifying opportunities for improvement. Am. J. Manag. Care 29 (7 Suppl), S104–S111. https://doi.org/10.37765/ajmc.2023.89390.

Mackenzie, I.R.A., Bigio, E.H., Ince, P.G., Geser, F., Neumann, M., Cairns, N.J., Kwong, L. K., Forman, M.S., Ravits, J., Stewart, H., Eisen, A., McClusky, L., Kretzschmar, H.A., Monoranu, C.M., Highley, J.R., Kirby, J., Siddique, T., Shaw, P.J., Lee, V.M.-Y., Trojanowski, J.Q., 2007. Pathological TDP-43 distinguishes sporadic amyotrophic lateral sclerosis from amyotrophic lateral sclerosis with SOD1 mutations. Ann. Neurol. 61 (5), 427–434. https://doi.org/10.1002/ana.21147.

Mandrekar, J.N., 2010. Receiver operating characteristic curve in diagnostic test assessment. J. Thorac. Oncol. 5 (9), 1315–1316. https://doi.org/10.1097/JTO.0b013e3181ec173d.

Martínez Gil, A., Dorronoso Díaz, I., Alonso Cascon, M., Panizo del Pliego, G., Fuertes Huerta, A., Pérez Puerto, M.J., Medina Padilla, M., 2005. WO2005097117A1.

Martínez-González, L., Gonzalo-Consuegra, C., Gómez-Almería, M., Porras, G., de Lago, E., Martín-Requero, Á., Martínez, A., 2021. Tideglusib, a non-ATP competitive inhibitor of GSK-3β as a drug candidate for the treatment of amyotrophic lateral sclerosis. Int. J. Mol. Sci. 22 (16). https://doi.org/10.3390/ijms22168975.

Masrori, P., Van Damme, P., 2020. Amyotrophic lateral sclerosis: a clinical review. Eur. J. Neurol. 27 (10), 1918–1929. https://doi.org/10.1111/ene.14393.

Miller, G., 1982. Immortalization of human lymphocytes by Epstein-Barr virus. Yale J. Biol. Med. 55 (3–4), 305–310.

Muti, P., Donzelli, S., Sacconi, A., Hossain, A., Ganci, F., Frixa, T., Sieri, S., Krogh, V., Berrino, F., Biagioni, F., Strano, S., Beyene, J., Yarden, Y., Blandino, G., 2018. MiRNA-513a-5p inhibits progesterone receptor expression and constitutes a risk factor for breast cancer: the hOrmone and Diet in the ETiology of breast cancer prospective study. Carcinogenesis 39 (2), 98–108. https://doi.org/10.1093/carcin/bgx126.

Nagaraj, S., Laskowska-Kaszub, K., Dębski, K.J., Wojsiat, J., Dąbrowski, M., Gabryelewicz, T., Kuźnicki, J., Wojda, U., 2017. Profile of 6 microRNA in blood plasma distinguish early stage Alzheimer's disease patients from non-demented subjects. Oncotarget 8 (10), 16122–16143. https://doi.org/10.18632/oncotarget.15109.

O'Brien, J., Hayder, H., Zayed, Y., Peng, C., 2018. Overview of microRNA biogenesis, mechanisms of actions, and circulation. Front. Endocrinol. 9, 402. https://doi.org/10.3389/fendo.2018.00402.

Oki, R., Izumi, Y., Fujita, K., Miyamoto, R., Nodera, H., Sato, Y., Sakaguchi, S., Nokihara, H., Kanai, K., Tsunemi, T., Hattori, N., Hatanaka, Y., Sonoo, M., Atsuta, N., Sobue, G., Shimizu, T., Shibuya, K., Ikeda, K., Kano, O., Kaji, R., 2022. Efficacy and safety of ultrahigh-dose methylcobalamin in early-stage amyotrophic lateral sclerosis: a randomized clinical trial. JAMA Neurol. 79 (6), 575–583. https://doi.org/10.1001/jamaneurol.2022.0901.

Pansarasa, O., Bordoni, M., Drufuca, L., Diamanti, L., Sproviero, D., Trotti, R., Bernuzzi, S., La Salvia, S., Gagliardi, S., Ceroni, M., Cereda, C., 2018. Lymphoblastoid cell lines as a model to understand amyotrophic lateral sclerosis disease mechanisms. Dis. Model. Mech. 11 (3). https://doi.org/10.1242/dmm.031625.

Posa, D., Martínez-González, L., Bartolomé, F., Nagaraj, S., Porras, G., Martínez, A., Martín-Requero, Á., 2019. Recapitulation of pathological TDP-43 features in immortalized lymphocytes from sporadic ALS patients. Mol. Neurobiol. 56 (4), 2424–2432. https://doi.org/10.1007/s12035-018-1249-8.

Prause, J., Goswami, A., Katona, I., Roos, A., Schnizler, M., Bushuven, E., Dreier, A., Buchkremer, S., Johann, S., Beyer, C., Deschauer, M., Troost, D., Weis, J., 2013. Altered localization, abnormal modification and loss of function of sigma receptor-1

in amyotrophic lateral sclerosis. Hum. Mol. Genet. 22 (8), 1581–1600. https://doi.org/10.1093/hmg/ddt008.
Requardt, M.V., Görlich, D., Grehl, T., Boentert, M., 2021. Clinical determinants of disease progression in amyotrophic lateral sclerosis-a retrospective cohort study. J. Clin. Med. 10 (8). https://doi.org/10.3390/jcm10081623.
Robinson, M.D., Smyth, G.K., 2008. Small-sample estimation of negative binomial dispersion, with applications to SAGE data. Biostatistics (Oxf., Engl.) 9 (2), 321–332. https://doi.org/10.1093/biostatistics/kxm030.
Robinson, M.D., McCarthy, D.J., Smyth, G.K., 2010. edgeR: a bioconductor package for differential expression analysis of digital gene expression data. Bioinformatics (Oxf., Engl.) 26 (1), 139–140. https://doi.org/10.1093/bioinformatics/btp616.
Sabatelli, M., Conte, A., Zollino, M., 2013. Clinical and genetic heterogeneity of amyotrophic lateral sclerosis. Clin. Genet. 83 (5), 408–416. https://doi.org/10.1111/cge.12117.
Sapaly, D., Cheguillaume, F., Weill, L., Clerc, Z., Biondi, O., Bendris, S., Buon, C., Slika, R., Piller, E., Sundaram, V.K., da Silva Ramos, A., Amador, M.D.M., Lenglet, T., Debs, R., Le Forestier, N., Pradat, P.-F., Salachas, F., Lacomblez, L., Hesters, A., Bruneteau, G., 2024. Dysregulation of muscle cholesterol transport in amyotrophic lateral sclerosis. Brain. https://doi.org/10.1093/brain/awae270.
Shannon, P., Markiel, A., Ozier, O., Baliga, N.S., Wang, J.T., Ramage, D., Amin, N., Schwikowski, B., Ideker, T., 2003. Cytoscape: a software environment for integrated models of biomolecular interaction networks. Genome Res. 13 (11), 2498–2504. https://doi.org/10.1101/gr.1239303.
Shellikeri, S., Karthikeyan, V., Martino, R., Black, S.E., Zinman, L., Keith, J., Yunusova, Y., 2017. The neuropathological signature of bulbar-onset ALS: a systematic review. Neurosci. Biobehav. Rev. 75, 378–392. https://doi.org/10.1016/j.neubiorev.2017.01.045.
Stanojlovic, M., Pang, X., Lin, Y., Stone, S., Cvetanovic, M., Lin, W., 2016. Inhibition of vascular endothelial growth factor receptor 2 exacerbates loss of lower motor neurons and axons during experimental autoimmune encephalomyelitis. PLoS One 11 (7), e0160158. https://doi.org/10.1371/journal.pone.0160158.
Sturmey, E., Malaspina, A., 2022. Blood biomarkers in ALS: challenges, applications and novel frontiers. Acta Neurol. Scand. 146 (4), 375–388. https://doi.org/10.1111/ane.13698.
Thul, P.J., Lindskog, C., 2018. The human protein atlas: a spatial map of the human proteome. Protein Sci. 27 (1), 233–244. https://doi.org/10.1002/pro.3307.
Tiwari, A., Sekhar, A.K.T., 2007. Workflow based framework for life science informatics. Comput. Biol. Chem. 31 (5–6), 305–319. https://doi.org/10.1016/j.compbiolchem.2007.08.009.
Vijayalakshmi, K., Ostwal, P., Sumitha, R., Shruthi, S., Varghese, A.M., Mishra, P., Manohari, S.G., Sagar, B.C., Sathyaprabha, T.N., Nalini, A., Raju, T.R., Alladi, P.A., 2015. Role of VEGF and VEGFR2 receptor in reversal of ALS-CSF induced degeneration of NSC-34 motor neuron cell line. Mol. Neurobiol. 51 (3), 995–1007. https://doi.org/10.1007/s12035-014-8757-y.
Waller, R., Bury, J.J., Appleby-Mallinder, C., Wyles, M., Loxley, G., Babel, A., Shekari, S., Kazoka, M., Wollff, H., Al-Chalabi, A., Heath, P.R., Shaw, P.J., Kirby, J., 2024. Establishing mRNA and microRNA interactions driving disease heterogeneity in amyotrophic lateral sclerosis patient survival. Brain Commun. 6 (1), fcad331. https://doi.org/10.1093/braincomms/fcad331.
Watanabe, S., Ilieva, H., Tamada, H., Nomura, H., Komine, O., Endo, F., Jin, S., Mancias, P., Kiyama, H., Yamanaka, K., 2016. Mitochondria-associated membrane collapse is a common pathomechanism in SIGMAR1- and SOD1-linked ALS. EMBO Mol. Med. 8 (12), 1421–1437. https://doi.org/10.15252/emmm.201606403.
Wojsiat, J., Laskowska-Kaszub, K., Mietelska-Porowska, A., Wojda, U., 2017. Search for Alzheimer's disease biomarkers in blood cells: hypotheses-driven approach. Biomark. Med 11 (10), 917–931. https://doi.org/10.2217/bmm-2017-0041.
Wu, X., Pan, Y., Fang, Y., Zhang, J., Xie, M., Yang, F., Yu, T., Ma, P., Li, W., Shu, Y., 2020. The biogenesis and functions of piRNAs in human diseases. Mol. Ther. Nucleic Acids 21, 108–120. https://doi.org/10.1016/j.omtn.2020.05.023.
Zhang, P., Lu, X., Shi, Z., Li, X., Zhang, Y., Zhao, S., Liu, H., 2019. miR-205-5p regulates epithelial-mesenchymal transition by targeting PTEN via PI3K/AKT signaling pathway in cisplatin-resistant nasopharyngeal carcinoma cells. Gene 710, 103–113. https://doi.org/10.1016/j.gene.2019.05.058.
Zhou, Y., Zhou, B., Pache, L., Chang, M., Khodabakhshi, A.H., Tanaseichuk, O., Benner, C., Chanda, S.K., 2019. Metascape provides a biologist-oriented resource for the analysis of systems-level datasets. Nat. Commun. 10 (1), 1523. https://doi.org/10.1038/s41467-019-09234-6.